

CURRENTS IN MONTEREY SUBMARINE CANYON

John Edward Hollister 18-74925

DODLEY KNOX LIBRARY  
NAVAL POSTGRADUATE SCHOOL  
MONTEREY, CALIFORNIA 93940

# NAVAL POSTGRADUATE SCHOOL

## Monterey, California



# THESIS

CURRENTS IN MONTEREY SUBMARINE CANYON

by

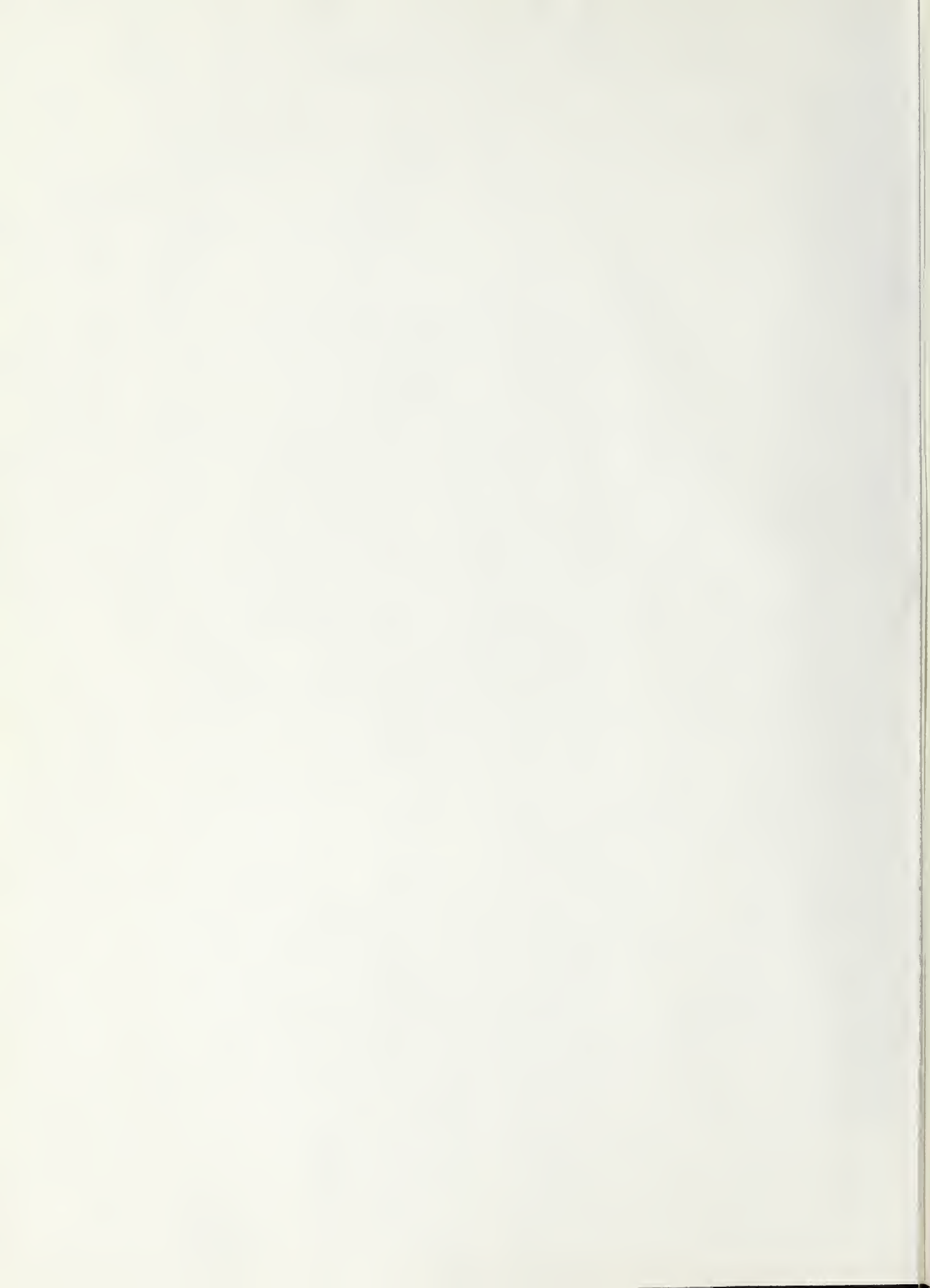
John Edward Hollister

September 1975

Thesis Advisors: R.S. Andrews & R.G. Paquette

Approved for public release; distribution unlimited.

T16980



Unclassified

SECURITY CLASSIFICATION OF THIS PAGE (When Data Entered)

REPORT DOCUMENTATION PAGE		READ INSTRUCTIONS BEFORE COMPLETING FORM
1. REPORT NUMBER	2. GOVT ACCESSION NO.	3. RECIPIENT'S CATALOG NUMBER
4. TITLE (and Subtitle)  Currents in Monterey Submarine Canyon		5. TYPE OF REPORT & PERIOD COVERED Master's Thesis; September 1975
		6. PERFORMING ORG. REPORT NUMBER
7. AUTHOR(s)  John Edward Hollister		8. CONTRACT OR GRANT NUMBER(s)
9. PERFORMING ORGANIZATION NAME AND ADDRESS  Naval Postgraduate School Monterey, California 93940		10. PROGRAM ELEMENT, PROJECT, TASK AREA & WORK UNIT NUMBERS
11. CONTROLLING OFFICE NAME AND ADDRESS  Naval Postgraduate School Monterey, California 93940		12. REPORT DATE September 1975
		13. NUMBER OF PAGES
14. MONITORING AGENCY NAME & ADDRESS (if different from Controlling Office)  Naval Postgraduate School Monterey, California 93940		15. SECURITY CLASS. (of this report)  Unclassified
		15a. DECLASSIFICATION/DOWNGRADING SCHEDULE
16. DISTRIBUTION STATEMENT (of this Report)  Approved for public release; distribution unlimited.		
17. DISTRIBUTION STATEMENT (of the abstract entered in Block 20, if different from Report)		
18. SUPPLEMENTARY NOTES		
19. KEY WORDS (Continue on reverse side if necessary and identify by block number)  Currents Submarine canyons Monterey Submarine Canyon		
20. ABSTRACT (Continue on reverse side if necessary and identify by block number)  Time series were obtained from two current meters near bottom on one mooring in Monterey Submarine Canyon. These records were analyzed to determine the general character of the currents, the volume transport at different levels above the canyon floor, the power spectral estimates of the up-canyon and cross-canyon directional components, and the coherence between directional components.		



Current speed variations appeared as a series of peaks occurring every 5 to 6 hr with maxima of 17 to 21 cm/sec. Current directions oscillated with a discernible period of about 12 hr. Currents 30 m above the bottom were aligned nearly along the canyon axis; currents 60 m above the bottom were nearly perpendicular to the canyon axis.

The spectral analysis indicated tides as a major driving force of the deep currents, but also indicated the presence of other forcing functions, possibly internal waves, with shorter periods. The coherence between instruments was low, suggesting the possible presence of a near-bottom boundary layer, or that significant signal deterioration was caused by noise.







Currents in Monterey Submarine Canyon

by

John Edward Hollister  
Lieutenant, United States Navy  
B.S., University of Hawaii, 1969

Submitted in partial fulfillment of the  
requirements for the degree of

MASTER OF SCIENCE IN OCEANOGRAPHY

from the

NAVAL POSTGRADUATE SCHOOL



## ABSTRACT

Time series were obtained from two current meters near bottom on one mooring in Monterey Submarine Canyon. These records were analyzed to determine the general character of the currents, the volume transport at different levels above the canyon floor, the power spectral estimates of the up-canyon and cross-canyon directional components, and the coherence between directional components.

Current speed variations appeared as a series of peaks occurring every 5 to 6 hr with maxima of 17 to 21 cm/sec. <sup>0.34 kw</sup> <sup>0.92 kw</sup> Current directions oscillated with a discernible period of about 12 hr. Currents 30 m above the bottom were aligned nearly along the canyon axis; currents 60 m above the bottom were nearly perpendicular to the canyon axis.

The spectral analysis indicated tides as a major driving force of the deep currents, but also indicated the presence of other forcing functions, possibly internal waves, with shorter periods. The coherence between instruments was low, suggesting the possible presence of a near-bottom boundary layer, or that significant signal deterioration was caused by noise.



## TABLE OF CONTENTS

I.	INTRODUCTION-----	11
A.	PURPOSE-----	11
B.	MONTEREY SUBMARINE CANYON-----	11
C.	PREVIOUS INVESTIGATIONS-----	12
II.	EQUIPMENT AND OBSERVATIONAL PROCEDURES-----	24
A.	CURRENT MEASURING SYSTEMS-----	24
1.	Geodyne A-100 Current Meter-----	24
2.	Hydro Products Model 502 Current Meter-----	26
B.	RELEASE MECHANISM-----	27
C.	CURRENT METER ARRAY-----	29
III.	DATA ANALYSIS-----	32
A.	SAMPLING RATES AND DIGITIZING PROCEDURES-----	32
B.	ELEMENTARY STATISTICS-----	33
C.	GRAPHIC DISPLAYS OF CURRENT METER DATA-----	34
1.	Histograms-----	34
2.	Scatter Diagrams-----	34
3.	Progressive Vector Diagrams-----	38
4.	Composite Drawings-----	38
D.	ALIASING-----	51
E.	HIGHER ORDER STATISTICS-----	51
IV.	DISCUSSION-----	52
A.	APPARENT CHARACTERISTICS-----	52
B.	SPECTRAL CHARACTERISTICS-----	56
V.	CONCLUSIONS-----	64



APPENDIX A: Program SUBMARINE CANYON-----	-66
APPENDIX B: Program VECTOR DRAW-----	-77
APPENDIX C: Program COMPOSITE DRAW-----	-80
REFERENCES-----	-83
INITIAL DISTRIBUTION LIST-----	-85





## LIST OF TABLES

I.	Canyon Current Statistics-----	18
II.	Mooring Statistics-----	31
III.	Elementary Current Statistics-----	53



## LIST OF FIGURES

1.	Monterey, Soquel, and Carmel Submarine Canyons-----	13
2.	Cross-sections of Monterey Submarine Canyon-----	14
3.	Locations of submarine canyons where current meter records have been obtained-----	16
4.	Format of 16-mm film output-----	25
5.	Encoding disk-----	25
6.	Format of strip chart output-----	28
7.	Current meter array-----	30
8.	Direction Histograms-----	35
9.	Scatter Diagram, 30 m above bottom-----	36
10.	Scatter Diagram, 60 m above bottom-----	37
11.	Progressive Vector Diagram, 30 m above bottom-----	39
12.	Progressive Vector Diagram, 60 m above bottom-----	40
13.	Progressive Vector Diagram, 30 m above bottom (expanded scale)-----	41
14.	Progressive Vector Diagram, 60 m above bottom (expanded scale)-----	42
15.	Composite Drawings, 29 Oct - 30 Oct-----	43
16.	Composite Drawings, 30 Oct - 31 Oct-----	43
17.	Composite Drawings, 31 Oct - 1 Nov-----	44
18.	Composite Drawings, 1 Nov - 2 Nov-----	44
19.	Composite Drawings, 2 Nov - 3 Nov-----	45
20.	Composite Drawings, 3 Nov - 4 Nov-----	45
21.	Composite Drawings, 4 Nov - 5 Nov-----	46
22.	Composite Drawings, 5 Nov - 6 Nov-----	46
23.	Composite Drawings, 6 Nov - 7 Nov-----	47



24.	Composite Drawings, 7 Nov - 8 Nov-----	47
25.	Composite Drawings, 8 Nov - 9 Nov-----	48
26.	Composite Drawings, 9 Nov - 10 Nov-----	48
27.	Composite Drawings, 10 Nov - 11 Nov-----	49
28.	Composite Drawings, 11 Nov - 12 Nov-----	49
29.	Composite Drawings, 12 Nov - 13 Nov-----	50
30.	Composite Drawings, 13 Nov - 14 Nov-----	50
31.	Directional Components versus Time, 30 m above bottom-----	57
32.	Directional Components versus Time, 60 m above bottom-----	58
33.	Power Spectral Estimate, Up-Canyon Component 60 m above bottom-----	59
34.	Power Spectral Estimate, Cross-Canyon Component 60 m above bottom-----	60
35.	Power Spectral Estimate, Up-Canyon Component 30 m above bottom-----	61
36.	Power Spectral Estimate, Cross-Canyon Component 30 m above bottom-----	62





## ACKNOWLEDGEMENT

The author gratefully acknowledges the following persons for their assistance in the preparation of this thesis: Professors Robert S. Andrews and Robert G. Paquette, co-advisors, for their support and advice; Sharon D. Raney of the NPS Computer Center for her hours of programming assistance; Jeannette C. Hollister for her help digitizing data and coding data sheets; the NPS Research Foundation for their generous funding of the research project; Woody Reynolds and the crew of the R/V ACANIA; and Dr. Francis P. Shepard for his time, advice, contributions of equipment, and inspiration.



## I. INTRODUCTION

### A. PURPOSE

The purpose of this study was to obtain further information about the near-bottom currents and current-related processes in Monterey Submarine Canyon such as turbidity currents, sediment transport, and internal waves. Some aspects of particular interest include: (i) the general character of currents within the canyon; (ii) volume transport at levels 30 m and 60 m above the canyon floor; (iii) power spectral estimates of current directional components; (iv) phase and coherence spectra between vector directional components from the two near-bottom current meters. These computations have not previously been made using time series approximately two weeks in length, obtained from deep portions of the canyon using vertically-arrayed current meters.

### B. MONTEREY SUBMARINE CANYON

Submarine canyons are typically rock walled, V-shaped winding valleys, with many dendritic tributaries, that extend seaward across the continental shelf and slope.

Monterey Canyon is the largest submarine canyon on the west coast of the United States, and heads near the center of Monterey Bay at Moss Landing. The canyon heads in unconsolidated sediment, but granite walls appear about 12.8 km seaward at depths of about 640 m..



The canyon is V-shaped, with high, steep walls and rocky outcrops, and has two major tributaries: Soquel Canyon entering from the north at a depth of 700 m and Carmel Canyon, which enters from the south at a depth of 1900 m (Fig. 1).

The gradient of the floor is on the order of 125 m/km in the upper reaches of the canyon. This decreases to 40 m/km at a depth of 91 m and thence remains fairly constant to depths of over 1,220 m [Shepard and Dill, 1966].

Further seaward Monterey Canyon loses its V-shaped walls, becoming broader and more trough-like. At an axial depth of 1,920 m the gradient decreases to 20 m/km, but high, steep walls continue out to a depth of 2,925 m. Here the true canyon terminates, <sup>44 nm</sup> 81.6 km from the canyon head, and becomes the wide, flat bottomed, levee-bordered Monterey Submarine Fan Valley. Cross-sections of the canyon at the investigation site, 1 km up-canyon and 1 km down-canyon from the investigation site, are shown in Fig. 2.

### C. PREVIOUS INVESTIGATIONS

Currents in submarine canyons off California were first measured in 1938 by Shepard, Revelle, and Dietz [1939]. These near-floor currents in the canyons off La Jolla, California, were observed to move alternately up-canyon and down-canyon, with variable periods. During numerous descents into the deep canyon in submersibles, Shepard [1967] observed currents moving both up and down the canyon axis with measured speeds of at least <sup>0.5 kn</sup> 25 cm/sec, fast enough to freely transport fine sand.



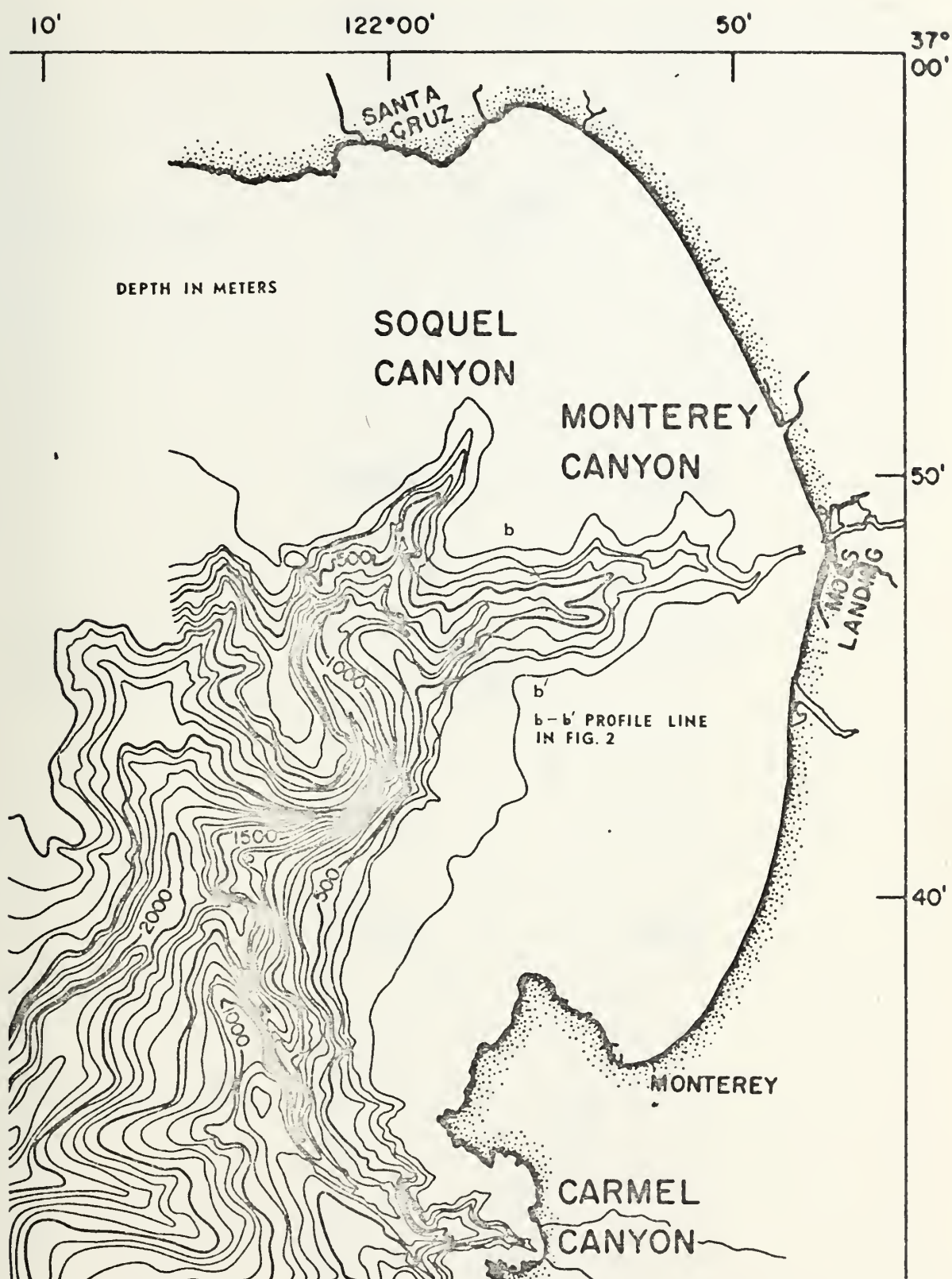
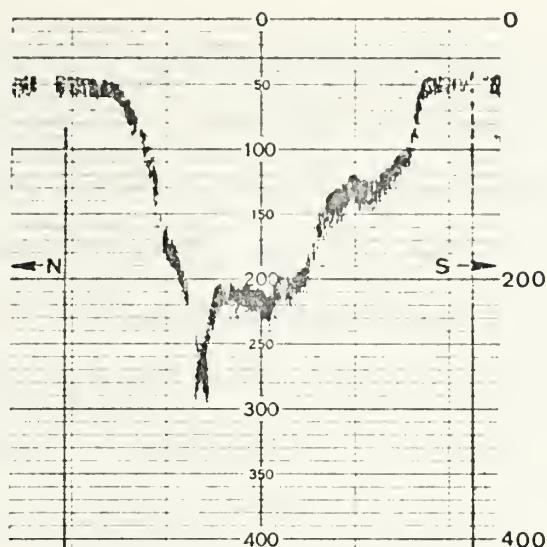


Fig. 1. Monterey, Carmel, and Soquel Submarine Canyons.  
[From Shepard and Dill, 1966]

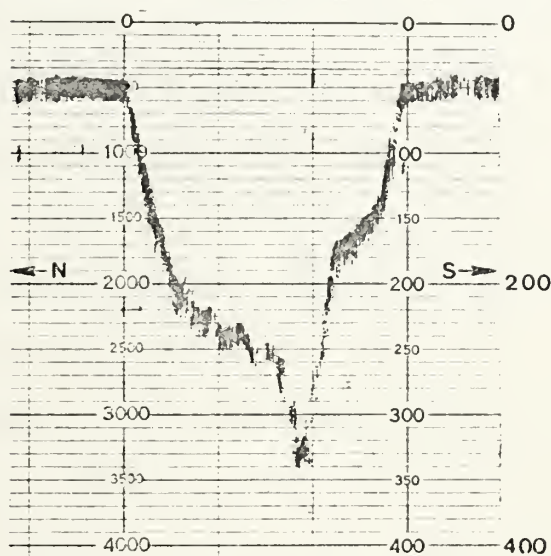




a. Up-canyon



b. Investigation Site



DEPTH IN FATHOMS

c. Down-canyon

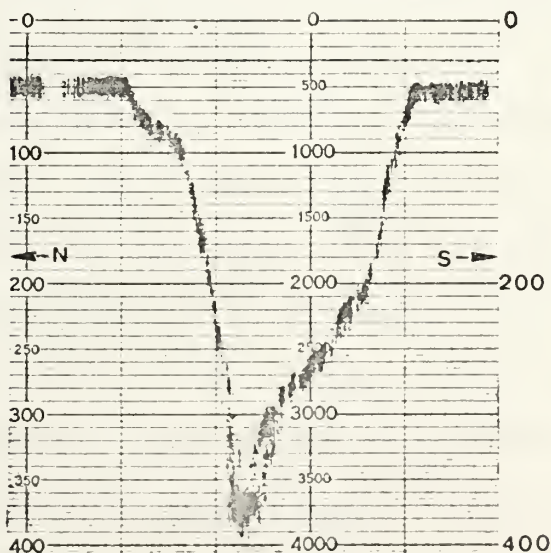


Fig. 2. Cross-sections of Monterey Submarine Canyon (Canyon width 4.4 km).



Indirect evidence of currents comes from photographs of ripple marks on the floors of canyons. In addition, evidence of recent rock erosion directly above the sediment fill on the canyon floors has been observed, such as polished wall rocks and overhanging cliffs, as well as down-canyon sediment creep.

Shepard and Marshall [1969] obtained a series of 3- to 6-day measurements from La Jolla Canyon indicating velocities up to 34 cm/sec with frequent oscillations in direction but far greater net down-canyon movement. No tidal relationships were readily discernible in these early records, but changes in flow from up-canyon to down-canyon were generally slow, virtually all of the higher speed currents occurred during ebb tides, and net water movement decreased with increasing distance above the canyon floor.

Shepard's continuing series of investigations have been conducted using Isaacs-Schick continuously recording Savonius-rotor type meters [Shepard and Marshall, 1969 and 1973b]. These meters were dropped from the surface into axes of submarine canyons and were held in position 3.6 m above the canyon floor by a heavy weight below and a group of floats above. The device was returned to the surface by the release of the bottom weight. Current meters were dropped into La Jolla Canyon at depths from 46 m to 375 m, San Lucas Canyon at 140 m, 220 m and 330 m, Newport Canyon at 100 m and 250 m, Redondo Canyon at 90 m and 250 m, Carmel Canyon at 160 m, and Monterey Canyon at 180 m (Fig. 3).

The canyon currents flowed predominantly in a direction that was parallel, or nearly parallel, to the axis of the



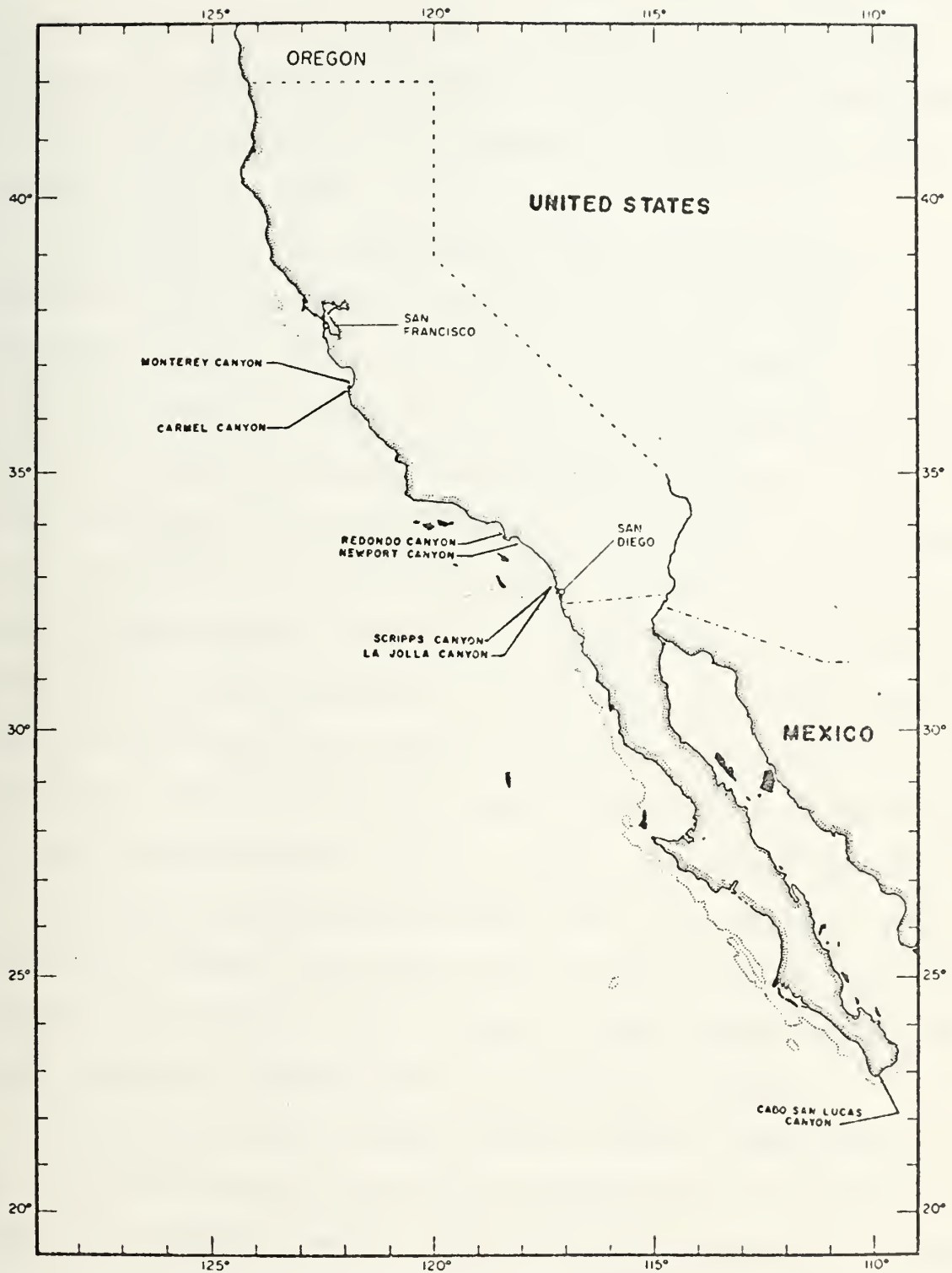


Fig. 3. Location of submarine canyons where current records have been obtained. [From Shepard and Marshall, 1973b]





canyon, and varying up-canyon or down-canyon. The steadiness of direction of up-canyon and down-canyon currents varied considerably from canyon to canyon. In general, however, down-canyon flow appeared to be steadier, perhaps because of its higher velocity (Table I).

The relation of up-canyon and down-canyon cycles to tidal periods is not yet clear, although some of the deeper stations recorded display cycles that are very nearly tidal in period (12 hr, 26 min). Attempts have been made [Shepard and Marshall, 1973b] to compare diurnal and semi-diurnal tides to see if this characteristic variation of Pacific tides has any influence on current cycles; records from a 206 m station in La Jolla Canyon show no appreciable change in the periodicity of flow reversal with the change in character of the tide. A 15-day record from the shallow station at Redondo Canyon was taken while passing through a spring period with semi-diurnal tides, then through a neap period with more nearly diurnal tides, and finally to a less marked spring semi-diurnal tide. The periods of current direction reversal for this record are far shorter than tidal periods and suggest the influence of some other forcing function, perhaps internal waves, at shallower depths.

A vertical array of three current meters above the bottom at the 206 m station in La Jolla Canyon provided information about the current profile. As previously mentioned, currents near the bottom showed a definitely tidal cycle for their peak flows. Currents 19 m and 34 m above the bottom showed similar periods of reversal, but had differing directions of flow.



Canyon Station	Canyon Location	Depth (Meters)	Number Successful Lowerings	Mean Velocity	Highest Velocity cm/sec	% time > 18 cm/sec		Net Transport Meters/hr		Total Directional Flow in Minutes		% Time Direct Flow		Average Length of flows (Min.)	
						Up	Down	Up	Down	Up	Down	Up	Down	Up	Down
1	La Jolla	46	2	1.07	26	.003	0	33.7	0	4,290	3,530	54.9	45.1	65.6	53.5
6	La Jolla	78	2	0.60	17	0	0	26.5	0	5,860	4,260	57.9	42.1	76.0	60.0
5	La Jolla	167	8	1.12	29	.017%	1.24%	0	37.1	20,810	24,090	46.4	53.6	75.0	94.0
3	La Jolla	206	14	2.51	29	.066%	3.23%	0	63.6	31,360	40,450	43.6	56.4	74.0	97.0
10	La Jolla	375	.2	2.08	22	1.29%	0.64%	0	15.8	5,840	6,700	46.5	53.5	216.0	247.0
9	Scrapps	125	2	0.85	34	0.65%	1.58%	0	13.9	4,190	5,870	41.6	58.4	47.0	63.0
14	San Lucas	137	3	0.86	17	0	0	0	29.4	2,850	5,540	33.9	66.1	12.0	23.0
13	San Lucas	216	1	0.44	9.5	0	0	0	13.6	1,770	2,890	28.6	71.4	18.0	28.0
15	San Lucas	328	2	3.70	33	0	6.20	0	123.1	2,870	7,190	38.0	62.0	30.0	71.0
20	Newport	101	2	0.92	17	0	0	0	34.1	2,345	2,960	44.1	55.9	87.0	105.0
21	Newport	252	1	0.16	11.5	0	0	0	0	1,010	1,530	39.7	60.2	168.0	255.0
18	Pedondo	92	2	1.97	27.0	.006	.011	0	34.2	8,275	12,112	41.5	58.5	87.4	114.9
19	Pedondo	283	1	3.19	19.0	.002	0	119.4	0	2,315	820	73.8	26.2	231.0	91.0
11	Carmel	156	1	3.36	20.0	0	0.28%	0	113.9	2,500	4,580	35.3	64.6	71.0	117.0
TOTALS						2.01	13.18	179.6	468.7	97,065	123,412			1313.0	1,467.0
AVERAGES						0.14	0.94	59.8	66.9	6,471	8,827	44.8	55.2	87.5	97.8

TABLE I. Canyon Current Statistics [from Shepard and Marshall, 1973b]



Net flow was decidedly down-canyon at the bottom, at right angles to the canyon at 19 m, and diagonal to the canyon at 34 m. If there is a level at which the direction is reversed, as is suggested by the spiraling directions reported, it appears to be at a height greater than 34 m above the bottom.

Evidence from pairs of stations in La Jolla, Santa Monica, Santa Cruz, Heuneme, Carmel, and Monterey Canyons exists [Shepard, Marshall, and McLaughlin, 1974b] to show internal waves being propagated along the canyon axes, and a close relationship in the direction of flow patterns at various heights above the canyon floors (up to 34 m) has been established. The evidence relating observed currents to internal waves includes the following: (i) the currents oscillate coherently at various heights above the bottom; (ii) the coherently oscillating systems advance along the canyons at velocities greater than the current velocities; (iii) the phase velocity is not correct for surface waves, but is the right order of magnitude for internal waves; (iv) similar types of currents and phase velocities occur on the continental shelf; (v) internal waves move up-canyon in all but one example, which is consistent with the general landward propagation of internal waves across the continental shelf.

By fitting together the current patterns at adjacent stations, displacing one station record relative to the other by a period of time proportional to the distance between the two stations, internal wave propagations speeds of 25 to 88 cm/sec have been calculated.



Although no relation between surface wind conditions and divergence of current flow from the canyon axes could be determined from early records, recent records show strong cross-canyon flows during periods of high cross-canyon wind. These cross-canyon surges also appear to have a tidally-influenced repetition cycle, and have highest speeds and longest durations in canyon areas with broad floors [Shepard, Marshall, and McLaughlin, 1974a].

Gatje and Pizinger [1965] made bottom current measurements in the head of Monterey Submarine Canyon in a water depth of 130 m utilizing an Ekman current meter placed 4.8 m above the bottom. Currents were observed to follow the canyon axes, with seaward flow on the rising tide and coastward flow on the falling tide. Current speed was sometimes fairly steady and other times variable, ranging between 0 and 41 cm/sec and with a median speed of <sup>0.2 kn</sup>10 cm/sec. During the 6-hr period centered around low tide the meters recorded currents that were, in general, considerably stronger than the currents recorded during the similar period of time centered around high tide.

An investigation of near-bottom currents in the head of Monterey Submarine Canyon was conducted by Dooley [1968] between March 1967 and May 1968. Continuous observations of water temperature, current speed, and direction were obtained over periods ranging from 5 hr to 162 hr using an internally recording Savonius-rotor current meter. Basic statistical parameters and power spectra were calculated for each record. These revealed an average current speed of about <sup>0.24 kn</sup>12 cm/sec







and current directions indicating flow reversals predominantly along the canyon axis. Current and water temperature oscillations indicated a strong semi-diurnal component. Water temperature changes also showed seasonal variation that agreed with the seasonal means of the region. Current speeds as high as <sup>1.0 km</sup> 52 cm/sec were recorded.

Njus [1968] made continuous bottom current measurements in the head of Monterey Submarine Canyon at water depths ranging from 146 to 201 m utilizing an internally recording Savonius-rotor current meter placed approximately 12 m above the bottom. Coincident wind, wave, and tide data were obtained along with the current measurements. Basic statistical parameters and power spectra were then computed for each time series. Current speeds in excess of <sup>1.0 km</sup> 52 cm/sec were measured, with the current direction being predominantly along the canyon axis. Water temperature, current speed and current direction all exhibited cyclic fluctuations with a periodicity of about 6 hr which, in a presentation of scalar speed, is approximately equal to that of the semi-diurnal tide. Warm, low-speed currents were reported flowing down-canyon on the rising tide. Even though this relation between tidal phase and current direction was also reported by Gatje and Pizinger [1965] it seems somewhat incongruous. One might expect an incoming tidal wave to cause a cold, up-canyon current, but not the opposite.

Average wind speeds were on the order of 10 kt (515 cm/sec) with a characteristic onshore/offshore diurnal variation



and did not appear to have any significant effect on the near-bottom currents. Wave conditions ranged from calm seas to wave periods of 20 sec and heights of about 0.6 m. The longer period, higher-amplitude waves appeared to increase the magnitude of current speeds, but this relationship was not examined in detail.

Caster [1969] measured near-bottom currents in Monterey Submarine Canyon and on the adjacent shelf using Savonius-rotor current meters. Simultaneous measurements were made with one current meter on the shelf at a depth of 91 m and one meter located in the canyon at <sup>1201 ft</sup> 366 m. Current speed, current direction and water temperature were recorded continuously for approximately 7 days in each record. Basic statistics were calculated and plotted for these time-series data. Scatter diagrams, progressive vector diagrams and power spectra were also computed and analyzed for the records collected during the study, and for available records of sufficient length from previous investigations.

Net transport was in a cross-canyon direction for many of the records; however, the currents in the canyon oscillated as reported in previous investigations. The oscillations were not as evident on the shelf record. Mean and maximum current speeds recorded in the canyon were <sup>1.6 cm</sup> 10 cm/sec and <sup>1.6 cm</sup> 51 cm/sec, respectively. On the shelf these values were <sup>0.14 cm</sup> 7 cm/sec and <sup>0.5 km</sup> 25 cm/sec, respectively. Observed values of net current direction and volume transport on the shelf appeared to be related to Monterey Bay seasonal water conditions.



Current direction was predominantly to the south during the oceanic period and latter part of the upwelling period; however, a northward set was observed during the transition period between the Davidson Current and upwelling periods. Volume transport values changed significantly from the oceanic period.

These earlier investigations have provided a description of the general character of the currents in submarine canyons, with which the results of this investigation may be compared. Most have reported a net down-canyon flow (Table I) and all have noted the tidally-influenced periodicity of flow reversal. Vertically arrayed current meters have recorded current speeds decreasing with distance above the bottom. Previous investigators have emphasized the along-axis components of the currents; cross-canyon components have been mentioned only briefly and spectral analyses, when performed, have not been thoroughly interpreted.



## II. EQUIPMENT AND OBSERVATIONAL PROCEDURES

### A. CURRENT MEASURING SYSTEMS

#### 1. Geodyne A-100 Current Meter

The Woods Hole Model A-100 Current Meter, manufactured by E.G. & G., Inc. (formerly Geodyne Corporation) in Waltham, Massachusetts, is a self-contained digital recording instrument measuring current direction and speed in the range from below 0.05 knots (2.6 cm/sec) to 5 knots (257 cm/sec) at depths to 6,000 m.

All data are recorded on 16-mm photographic film. The power required is provided by a special 6-volt battery pack, and the record consists of 100 ft of film which permits 5,000 sets of rotor speed, vane, and compass direction readings. The current speed sensor is a Savonius rotor; the vane, which is part of the direction system, is read digitally along with an internal magnetic compass. The film can either be run continuously for 6.5 days or programmed to record currents intermittently for up to a year.

A segment of the 16-mm film output is shown in Fig. 4. The seven intermittent black streaks on the left of the film, following the first continuous streak, show the orientation of the vane relative to a fixed direction within the instrument. The next seven streaks show the orientation of a compass relative to a fixed direction within the instrument. These streaks are made by points of light, transmitted via optical





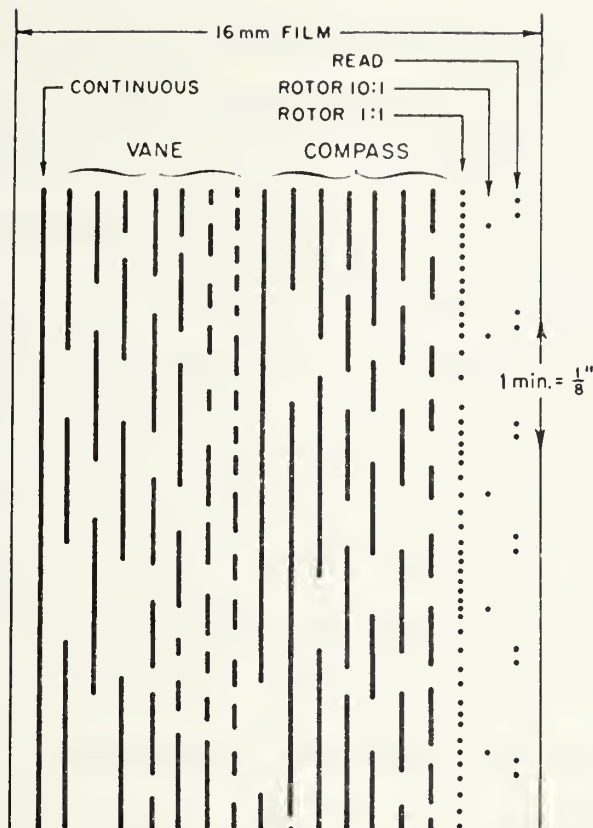


Fig. 4. Format of 16-mm film output. [From Richardson, Stimson, and Wilkins, 1963]

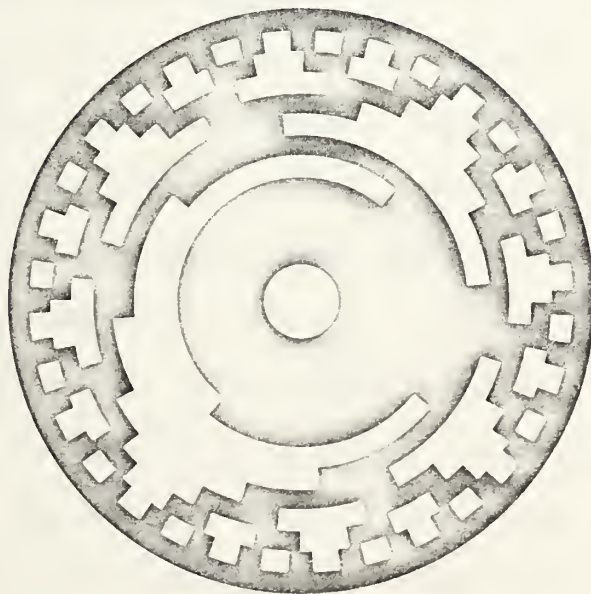


Fig. 5. Encoding disk. [From Richardson, Stimson, and Wilkins, 1963]



fibers, that reach the film as permitted by the encoding disk shown in Fig. 5. The encoding disk is associated with both the vane recording and compass recording systems. Each of the two angles measured by this system can be resolved to  $2.5^{\circ}$  and the combination of the two angles provided the direction of the current referred to magnetic North.

Each time the Savonius rotor of the meter goes around once, a black dot occurs in the first current channel; ten revolutions causes a dot in the next channel. At times, the rotor is turned so rapidly that the dots in the first channel are too close to be resolved; when this happens the second channel provides current speed information. Timing marks are provided in the last channel [E.G.& G., undated].

## 2. Hydro Products Model 502 Current Meter

The Model 502 In-Situ Recording System, manufactured by Hydro Products in San Diego, California, is a self-contained instrument package which measures and records current speed, current direction, and temperature. The underwater speed sensor is a Savonius rotor. Water movement past the sensor turns the rotor at an angular rate proportional to the speed of the flow. Ten magnets attached to the rotor close a magnetic reed switch which is in series with a DC voltage source. The output from the sensor is a pulse train whose rate is proportional to the angular rate of the rotor and therefore proportional to the current speed. The rate is measured with a simple rate-meter circuit.



The current direction sensor consists of a microtorque potentiometer and compass. Current direction is measured with reference to magnetic North. The vane of the direction sensor is magnetically connected to the slider of the potentiometer, which is attached to the compass. When the potentiometer is energized by a d.c. voltage, the voltage output on the slider is proportional to its angle of deflection from magnetic North [Hydro Products, undated].

The electronics circuitry, battery, clock timer, and a Rustrak strip chart recorder are contained in an aluminum sphere. The Rustrak recorder incorporates a switching system that allows the three separate parameters to be recorded sequentially as a function of time. The recording cycle is 7.5 min long; speed and temperature are recorded alternately at 4-sec intervals for 1.5 min followed by a 5-min record of speed and direction. The timer starts a new 7.5-min recording cycle every half-hour.

An example of the display obtained is shown in Fig. 6. The three functions are easily identified by the length of the imprint lines of the chart paper.

## B. RELEASE MECHANISM

A timed release mechanism manufactured by the Braincon Corporation of Marion, Massachusetts, was used to return the current meter array to the surface. A quartz timer and electronics from a Model 622 release was housed in a Model 422 pressure case. When the timer counts to zero from a preset number, an explosive squib is fired releasing a cocking



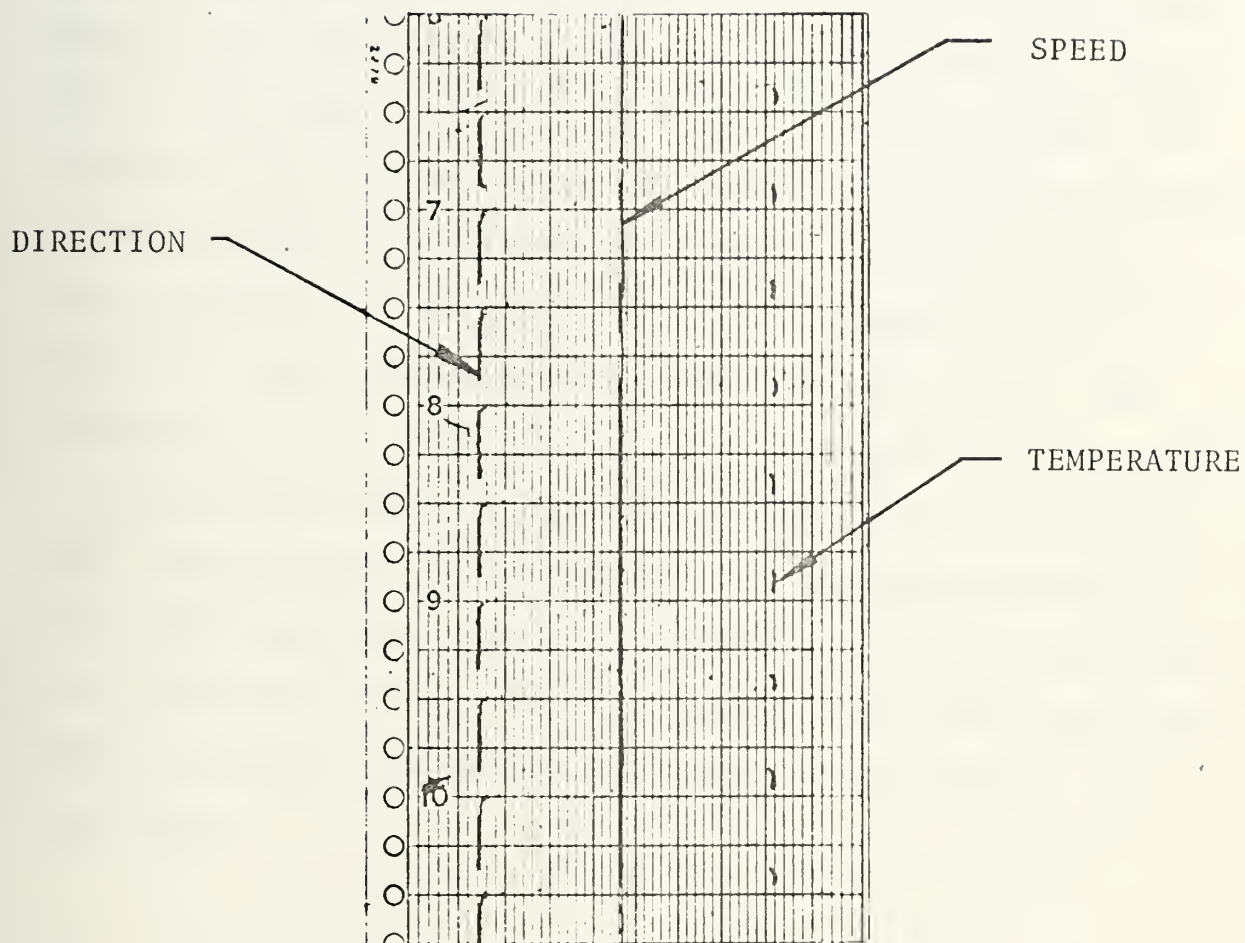


Fig. 6. Format of strip chart output.  
[From Hydro Products, undated]





pawl which then allows the mechanism to separate from the anchor.

### C. CURRENT METER ARRAY

All instruments used in this investigation were calibrated before deployment, either at the factory or using procedures specified in the operating manual. The array used to deploy the current meters is shown in Fig. 7. Three moorings were attempted but only one array was recovered. The successfully recovered array was deployed in Monterey Submarine Canyon in 485 m of water at position  $36^{\circ} 47.5'N$  latitude,  $121^{\circ} 54.2'W$  longitude, approximately 9.6 km WSW of Moss Landing. The statistics of the three moorings are summarized in Table II.

Due to the length of the array, an "anchor-last" deployment was made from the R/V ACANIA. As the emplacement site was approached, the array was streamed behind the ship, buoys first, with the anchor retained aboard. After the emplacement site was passed, the anchor was dropped and the array sank into place.



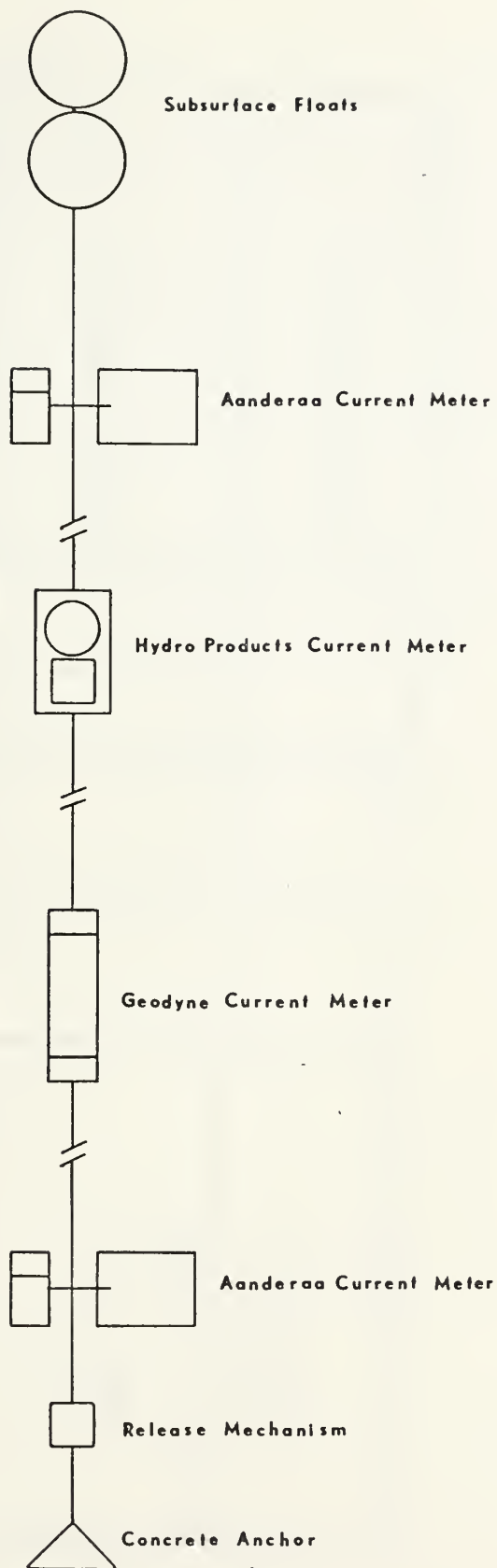


Fig. 7. Current meter array.



Station Location & Depth	Height Above Bottom	Record Length	Remarks
36° 47.5' N 121° 54.2' W <i>1591 ft</i> 485 m	425 m 60 m 30 m 3 m	0 371 hr 262 hr 0	Pressure case flooded Directions for 342 hr Electronics malfunction
36° 46.0' N 121° 57.8' W <i>1591 ft</i> 767 m	707 m 60 m 30 m 3 m	0 0 0 0	Release Failure
36° 47.5' N 121° 54.2' W 485 m	30 m 10 m	0 0	Release Failure

TABLE II. Mooring Statistics



### III. DATA ANALYSIS

#### A. SAMPLING RATES AND DIGITIZING PROCEDURES

The Geodyne A-100 current meter was programmed to sample speed and direction for 50 sec at 5-min intervals. The developing and printing of the current meter film was handled by E.G. & G., Environmental Equipment Division. An automatic film reader was then used to convert the Grey binary code on the film into digital form. This output was subsequently transferred to punched computer cards.

A characteristic of the computer program associated with the automatic film reader is that if the current meter records a speed below that designated as the threshold of sensitivity for the instrument an "implied zero" is printed. Since it is unlikely that currents in the canyon are really zero for any significant length of time, a value of 1.54 cm/sec, approximately half the threshold speed, was substituted for the implied zero value. This accounts for the apparent "floor" seen in the speed versus time graphs of the 30 m above-bottom record.

When employing the Hydro Products Model 502 current meter one must choose between a continuous record with a 7-day data storage capacity, or a 30-min sampling interval with a 30-day recording life. Since a long time series was desired, the 30-min sampling interval was selected. This rate was frequent enough to describe long period variations, but may have been





insufficient to fully describe high frequency variations of speed and direction. The resulting aliasing problem is discussed later in this section.

The analog strip chart data was digitized at 30-min intervals using calibration plates supplied with the instrument and the resulting numbers punched onto computer cards.

## B. ELEMENTARY STATISTICS

Program SUBMARINE CANYON (Appendix A), an extensive modification of a program written by Dooley [1968], was used to compute the basic statistics of the current meter data, as listed below.

The outputs from SUBMARINE CANYON include:

- (1) hourly means,
- (2) daily means, medians, modes, and frequency distributions, and
- (3) time series means, medians, modes, standard deviations, and direction histograms.

Average speed is defined as a simple arithmetic mean. For  $N$  speed observations,  $V_i$ , the average is defined as:

$$\bar{V} = \frac{1}{N} \sum_{i=1}^N V_i \quad \text{average speed}$$

However, to give more physical meaning to an average velocity a vector average, obtained by using the mean north and east components as shown below, is used to define an average direction:

$$\bar{V}_e = \frac{1}{N} \sum_{i=1}^N (V_i \sin \theta_i) \quad \text{average east component}$$



$$\bar{V}_n = \frac{1}{N} \sum_{i=1}^N (V_i \cos \theta_i) \quad \text{average north component}$$

$$\bar{\theta} = \arctan \left( \frac{\bar{V}_e}{\bar{V}_n} \right) \quad \text{average direction}$$

where  $\theta_i$  is the  $i^{\text{th}}$  direction observation.

## C. GRAPHIC DISPLAYS OF CURRENT METER DATA

### 1. Histograms

The direction histograms (Fig. 8a and 8b) are also an output of SUBMARINE CANYON. The range of directions is divided into  $10^0$  intervals and the frequency of occurrence of directions within each interval is computed and plotted. The most common values of direction and the variances about them are readily determined by examination of the histograms.

It is physically misleading, however, to interpret the independent modal values of direction as a description of an average velocity vector; the directions plotted do not use coincident current speeds as weighting factors and therefore do not accumulate to a vector average. Vector scatter diagrams are more indicative of flow direction.

### 2. Scatter Diagrams

Scatter diagrams (Fig. 9 and 10) are used to complement the histograms. These polar plots of the current vectors clearly associate speeds with directions and give a more precise physical meaning to the bi-modal character of the flow suggested by the direction histograms. However, because large vectors obscure small ones, this type of presentation is



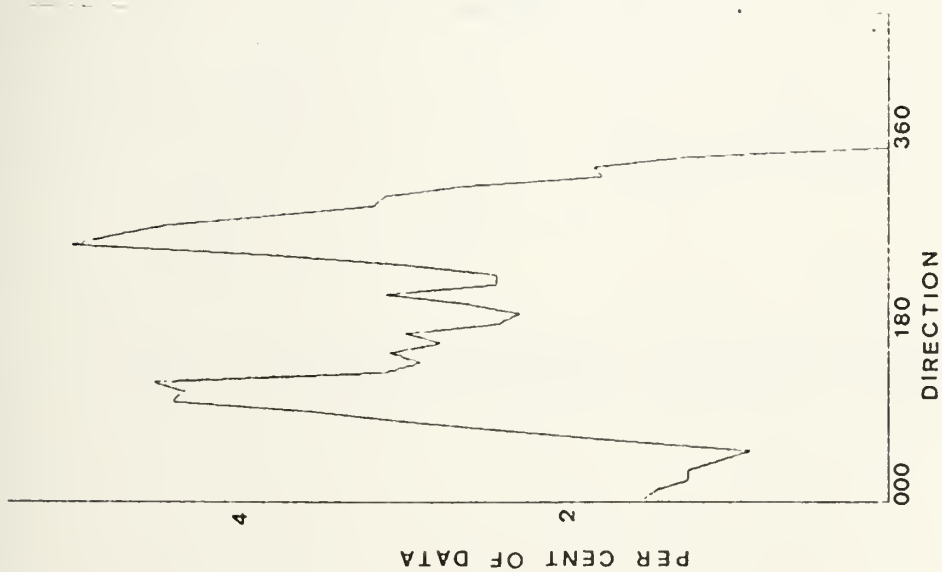


Fig. 8a. Direction Histogram,  
30 m above bottom

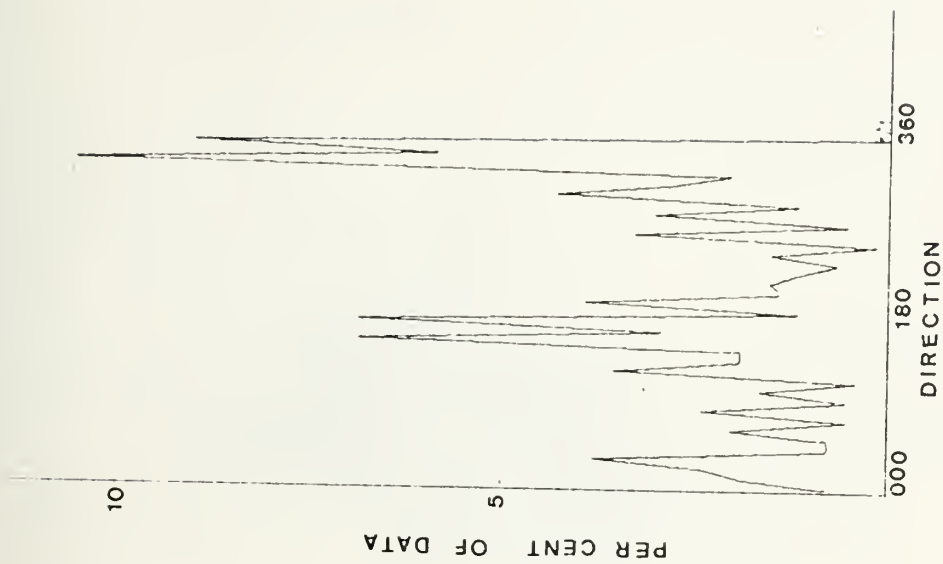


Fig. 8b. Direction Histogram,  
60 m above bottom



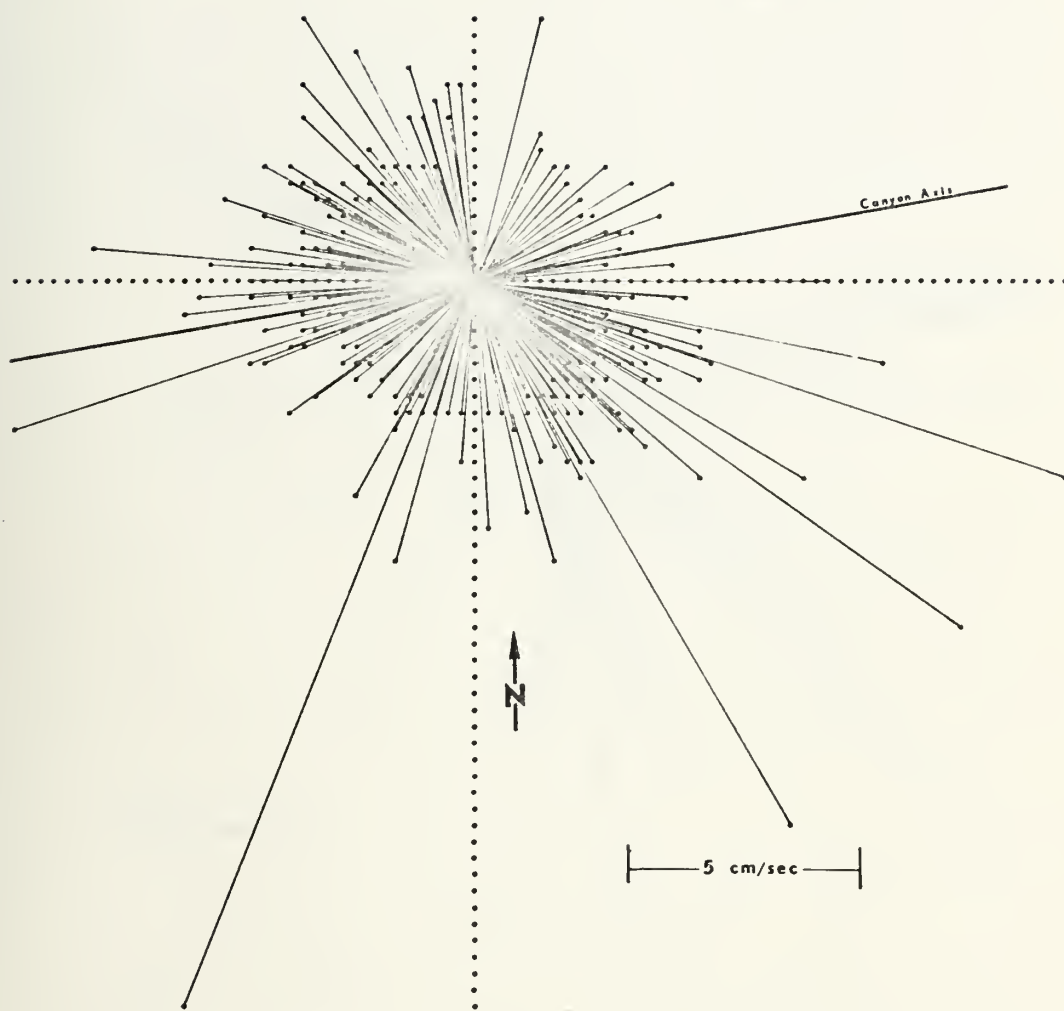


Fig. 9. Scatter Diagram, 30 m above bottom.





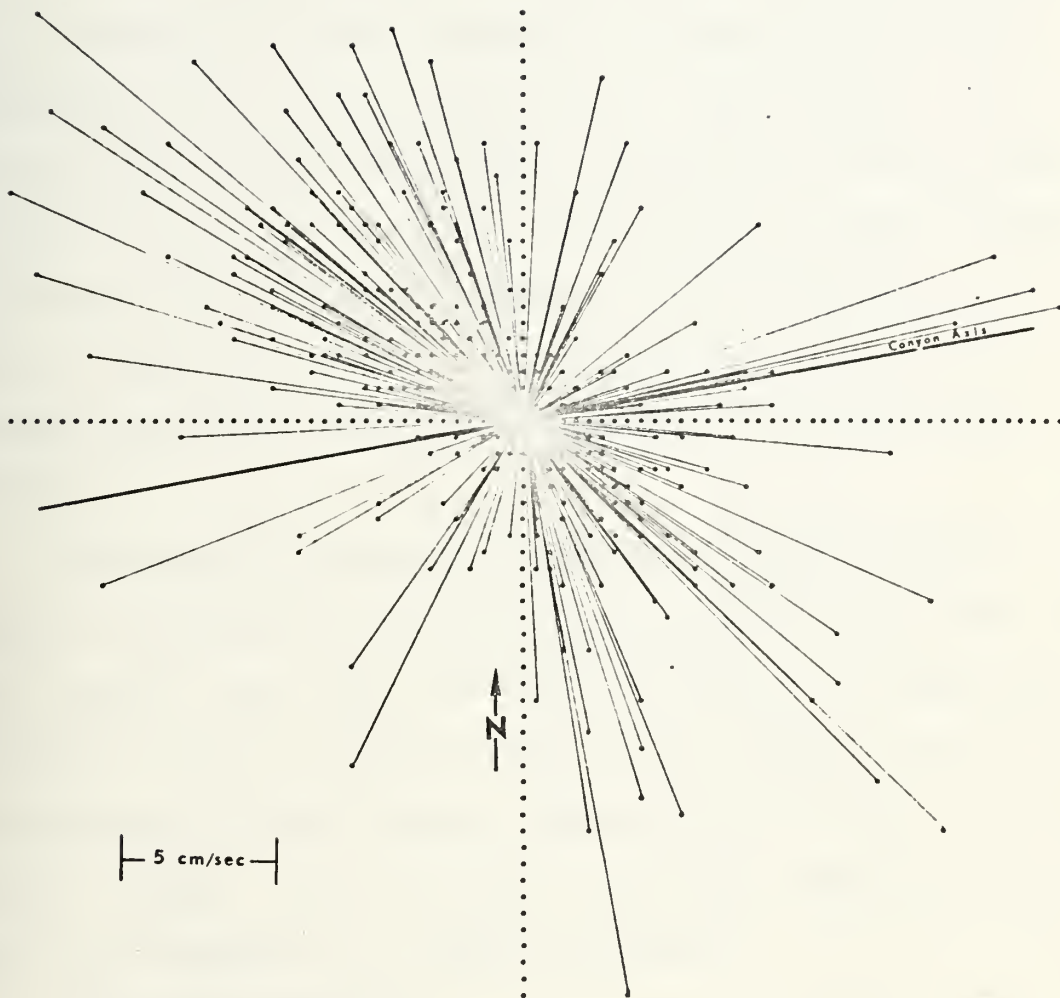


Fig. 10. Scatter Diagram, 60 m above bottom.



also imperfect. Progressive vector diagrams must be examined to obtain some measure of the net flow.

### 3. Progressive Vector Diagrams

Vector displacement, or progressive vector diagrams (Fig. 11 through 14) are convenient methods of graphically representing time series current meter observations. They are useful for quickly portraying the mean flow and the general character of low frequency--particularly rotary--changes, and also put high frequency changes into perspective as to magnitude [Webster, 1964a]. The diagram is constructed by computing the vector sum of displacements over given time intervals.

Although the progressive vector diagram resembles a particle trajectory, it is unwise to think of it as such. Only in the special case where the field of motion is independent of position over the spatial scale of the summed vectors would the progressive vector diagram represent a particle trajectory [Webster, 1964b]. It is unlikely that this condition exists within the confines of a submarine canyon.

### 4. Composite Drawings

Current speeds and directions were plotted versus time in 24-hr increments for the entire time series. In these graphs (Fig. 15 through 30), which were generated by program COMPOSITE DRAW (Appendix B), the general character of the fluctuations of the parameters may be ascertained. The directions 60 m above bottom never go through  $360^{\circ}$ , so direction rotations cannot be seen. This is due to the sampling procedure



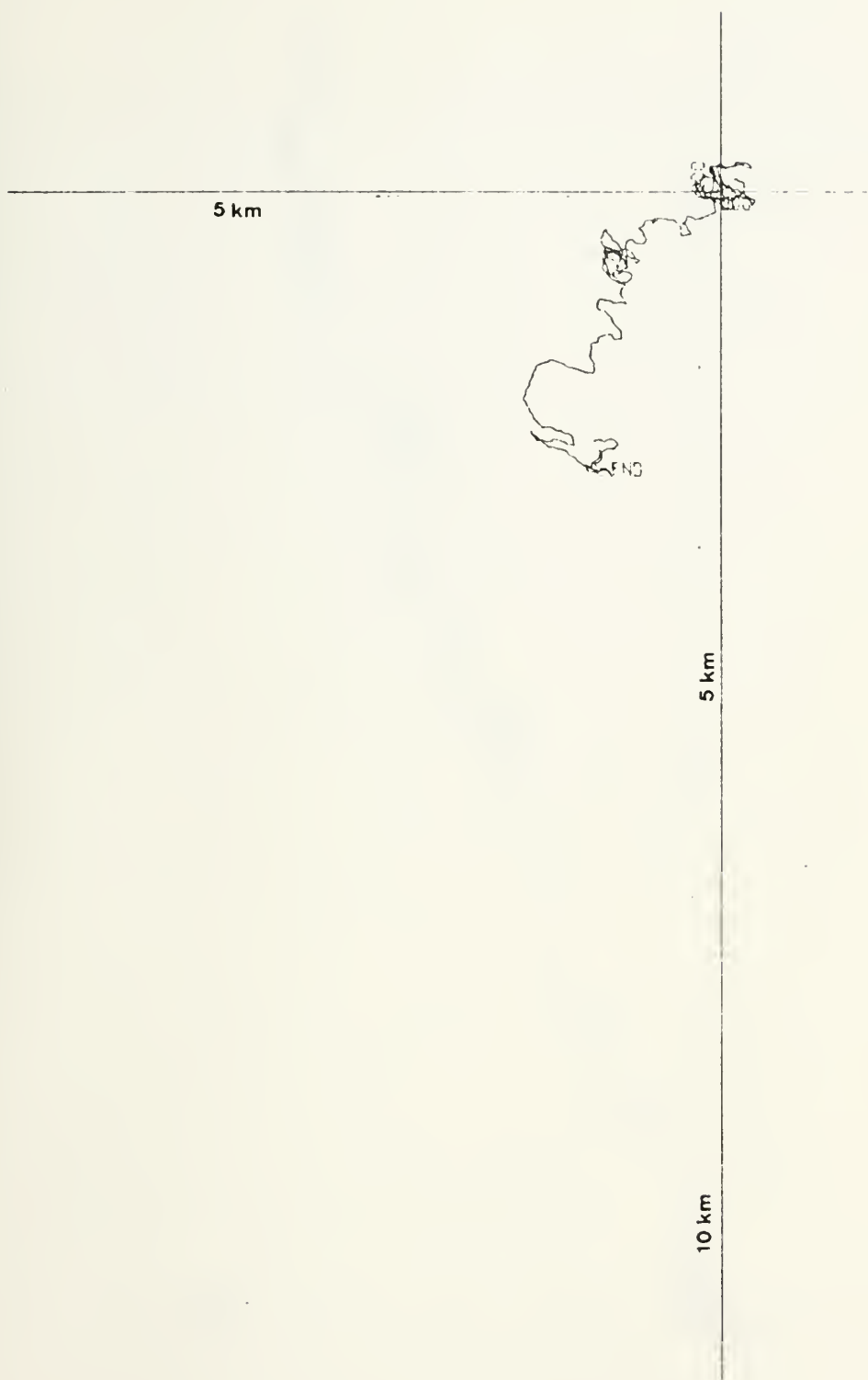


Fig. 11. Progressive Vector Diagram,  
30 m above bottom.



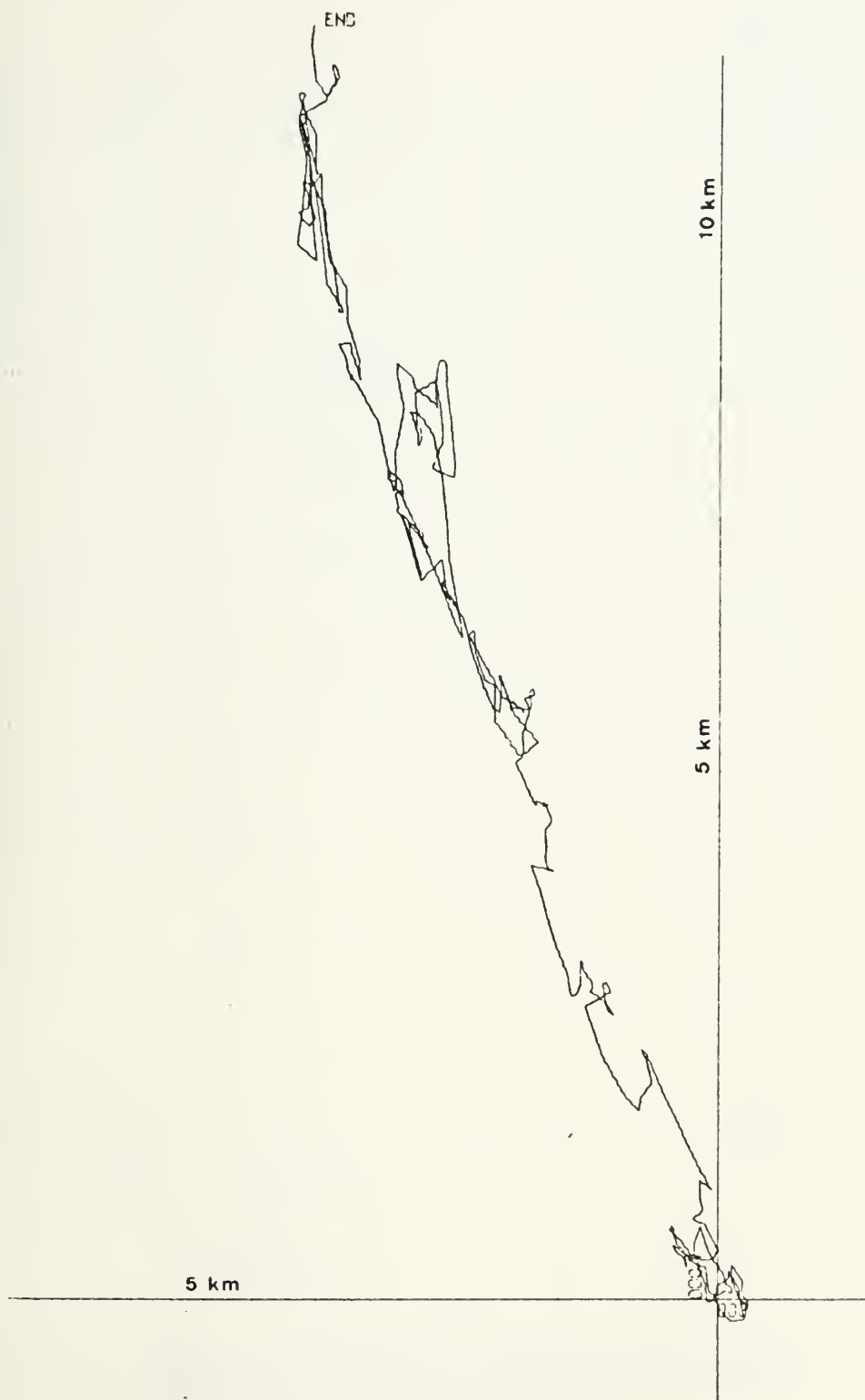


Fig. 12. Progressive Vector Diagram,  
60 m above bottom.







Fig. 13. Progressive Vector Diagram, 30 m above bottom (expanded scale). Successive 24-hr periods marked by "X".



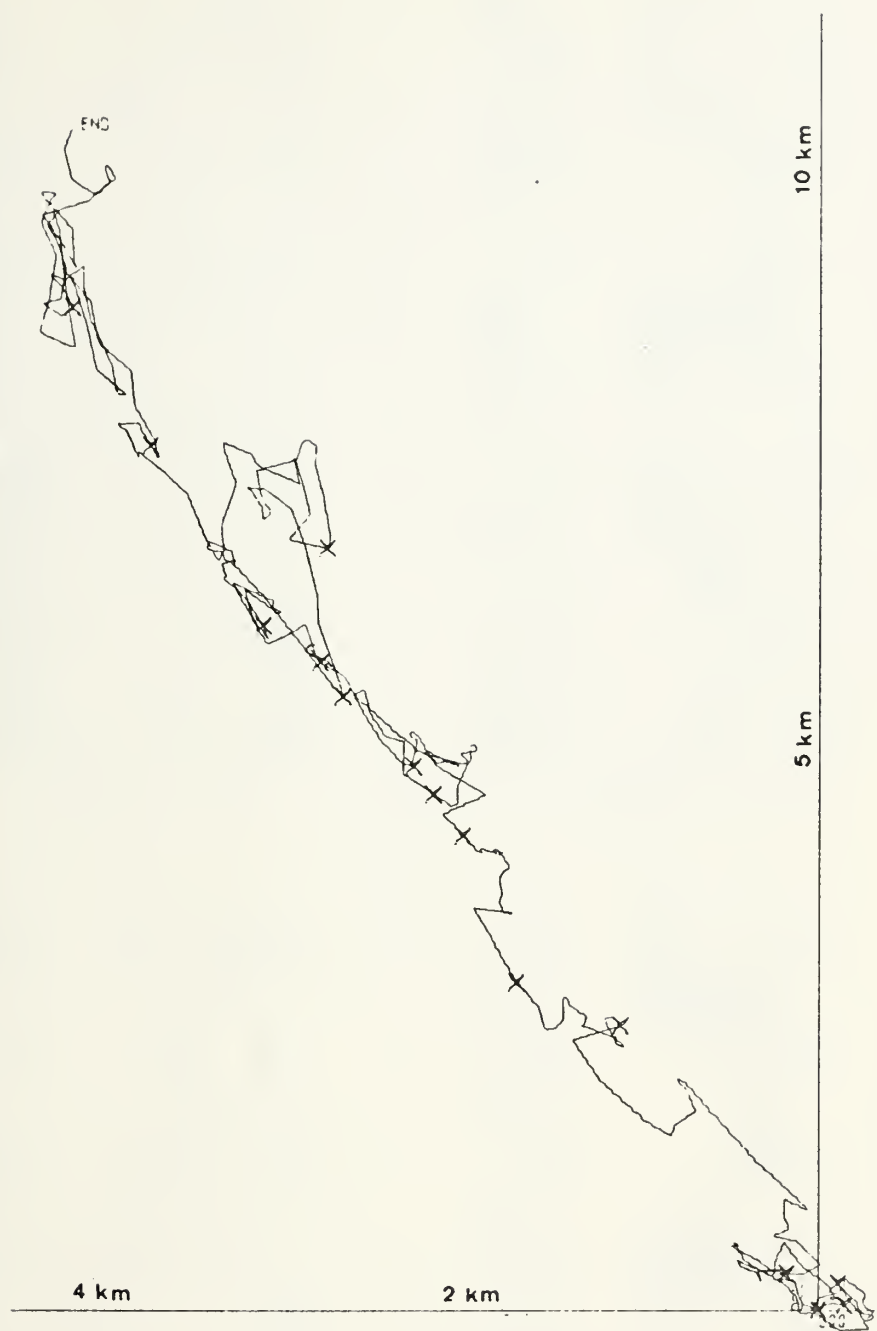


Fig. 14. Progressive Vector Diagram, 60 m above bottom (expanded scale). Successive 24-hr periods marked by "X".



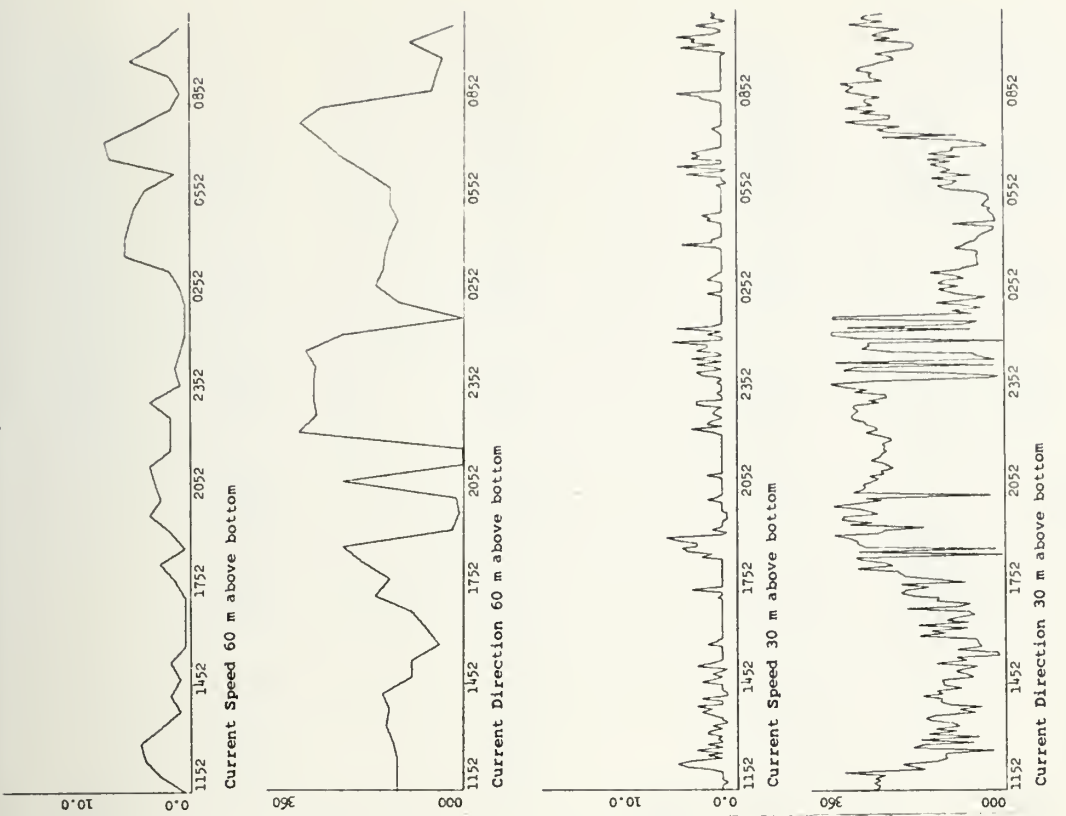


Fig. 15. Composite Drawings,  
29 Oct - 30 Oct

(Fig. 15-30, speeds in cm/sec; time is PDT)

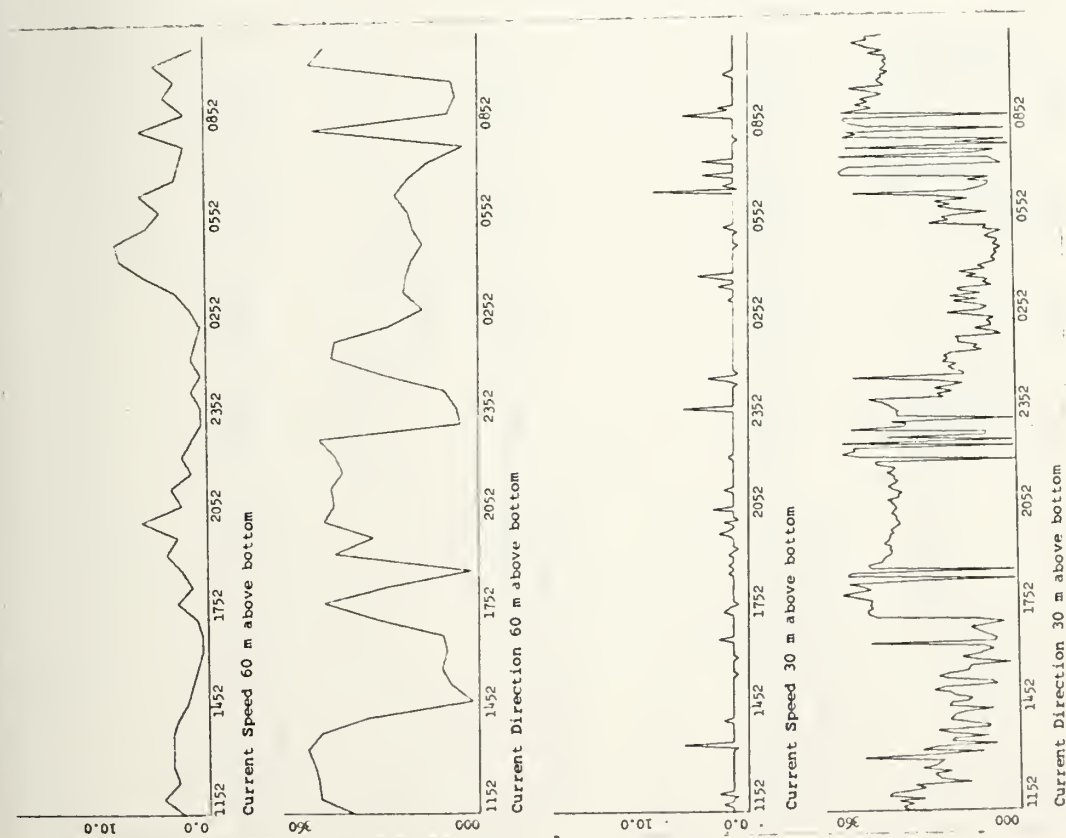


Fig. 16. Composite Drawings,  
30 Oct - 31 Oct



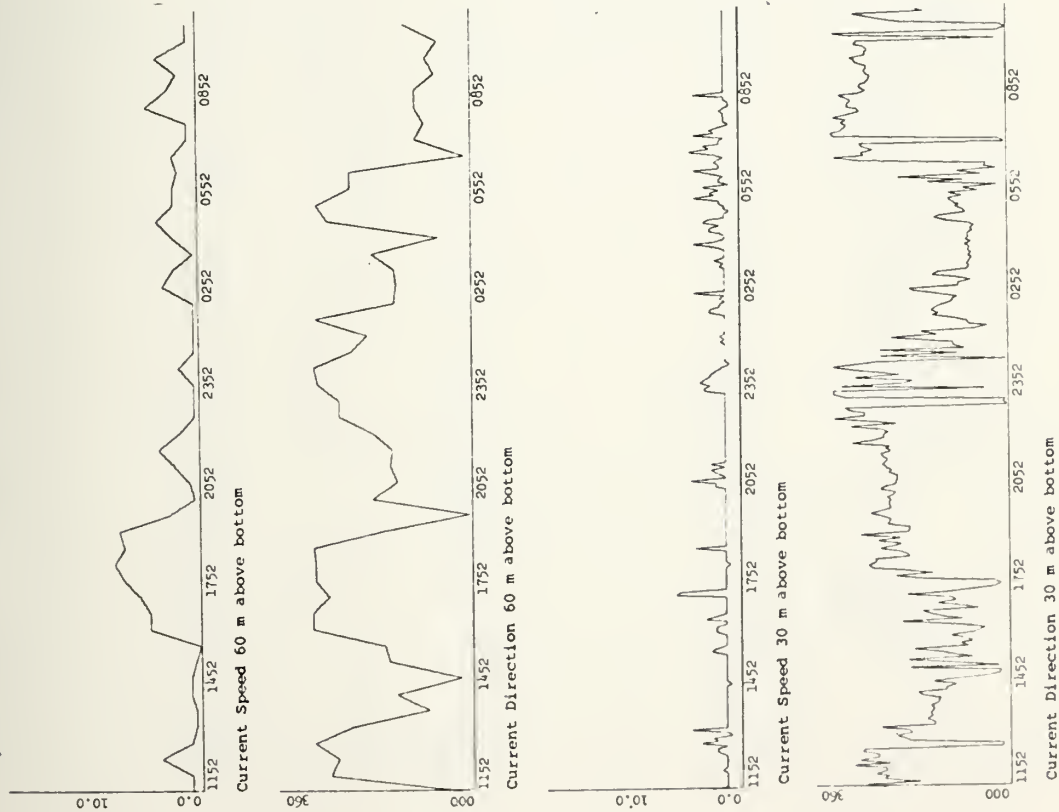


Fig. 17. Composite Drawings,  
31 Oct - 1 Nov

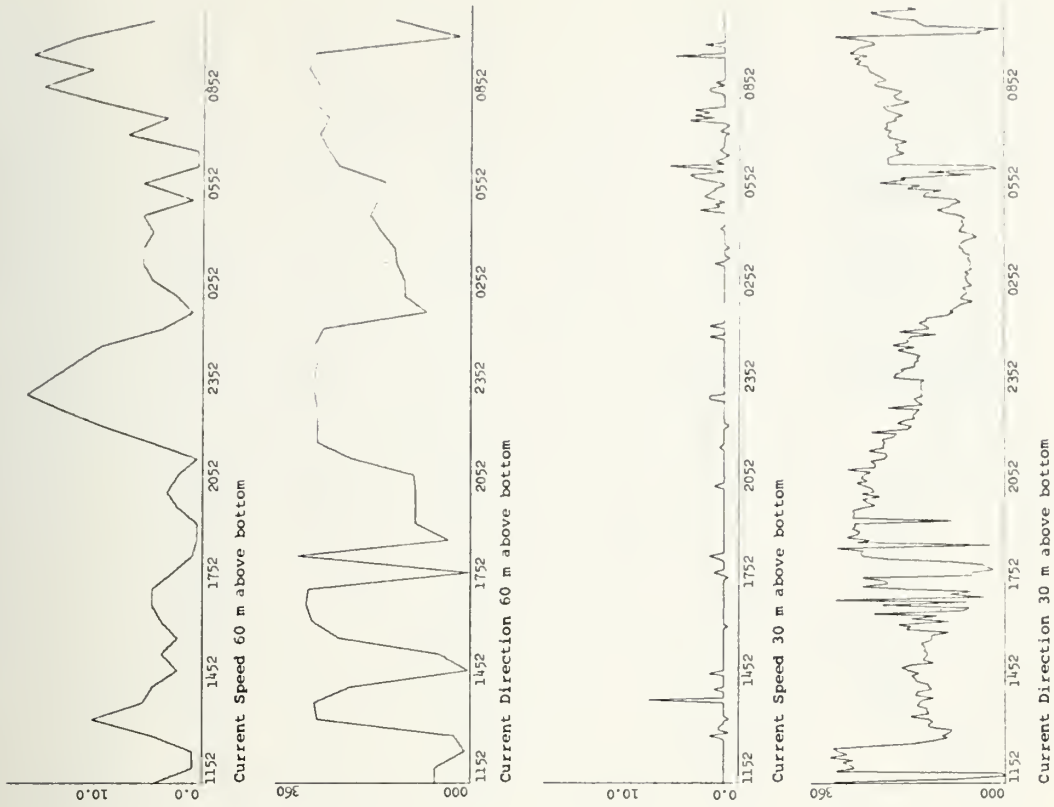


Fig. 18. Composite Drawings,  
1 Nov - 2 Nov





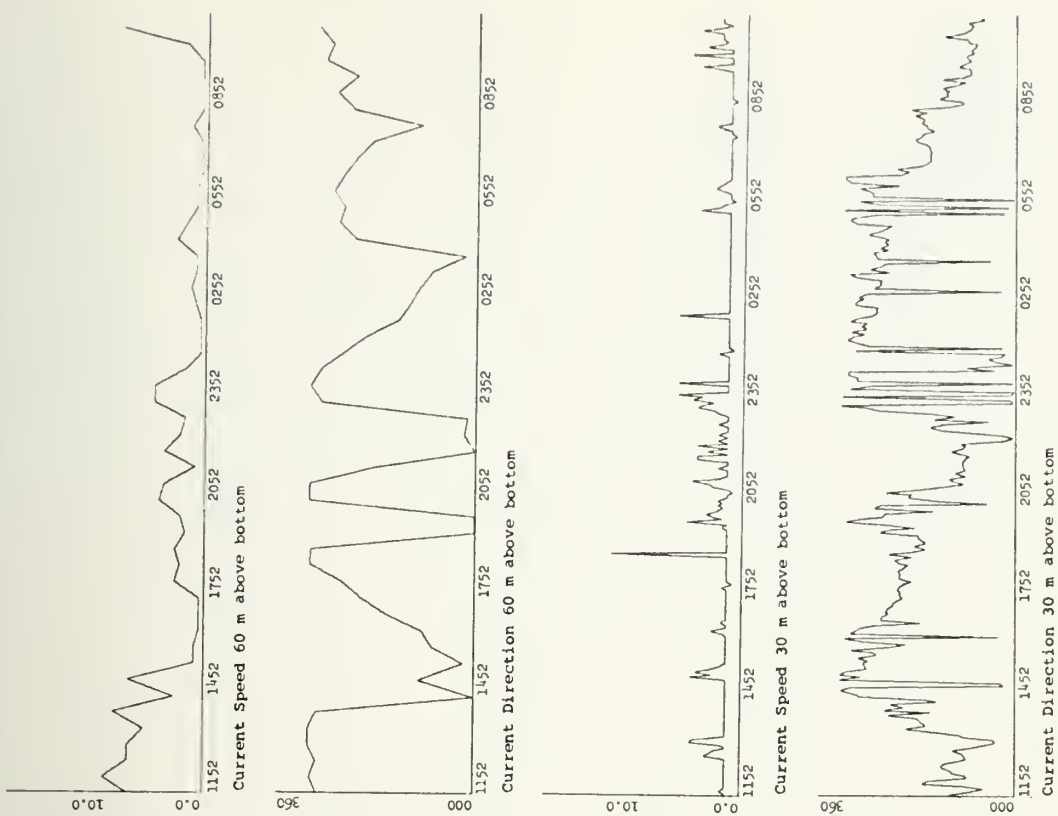


Fig. 19. Composite Drawings,  
2 Nov - 3 Nov

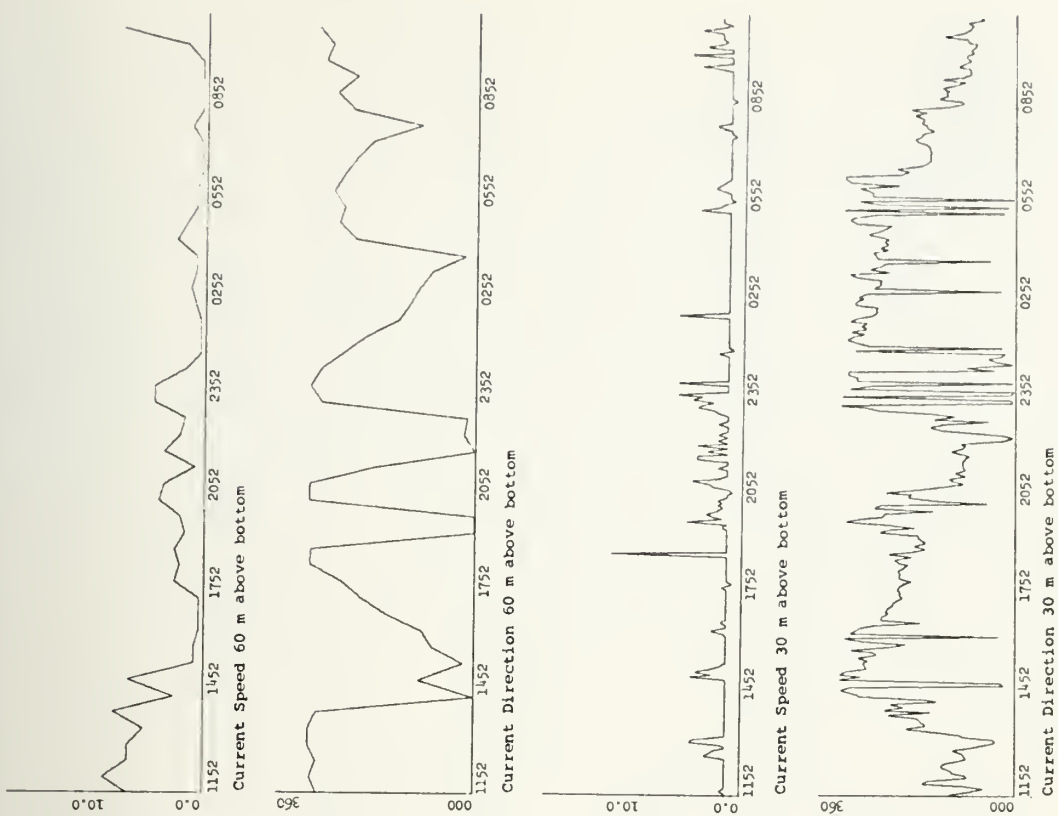


Fig. 20. Composite Drawings,  
3 Nov - 4 Nov



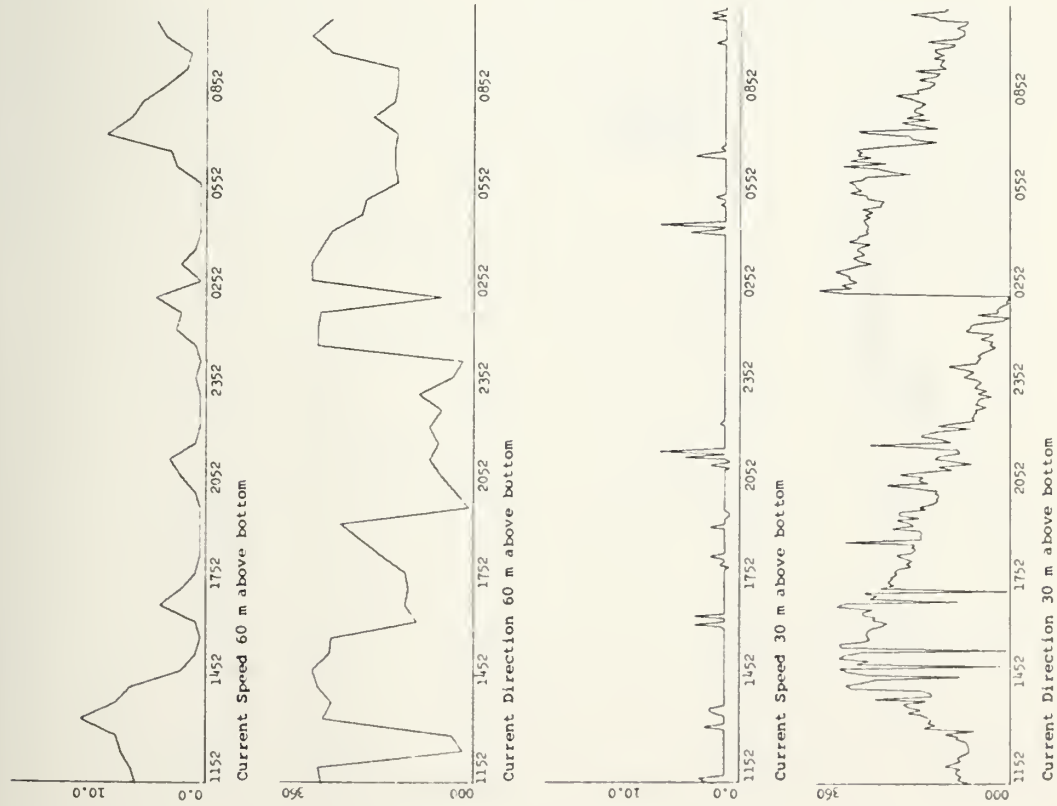


Fig. 21. Composite Drawings,  
4 Nov - 5 Nov

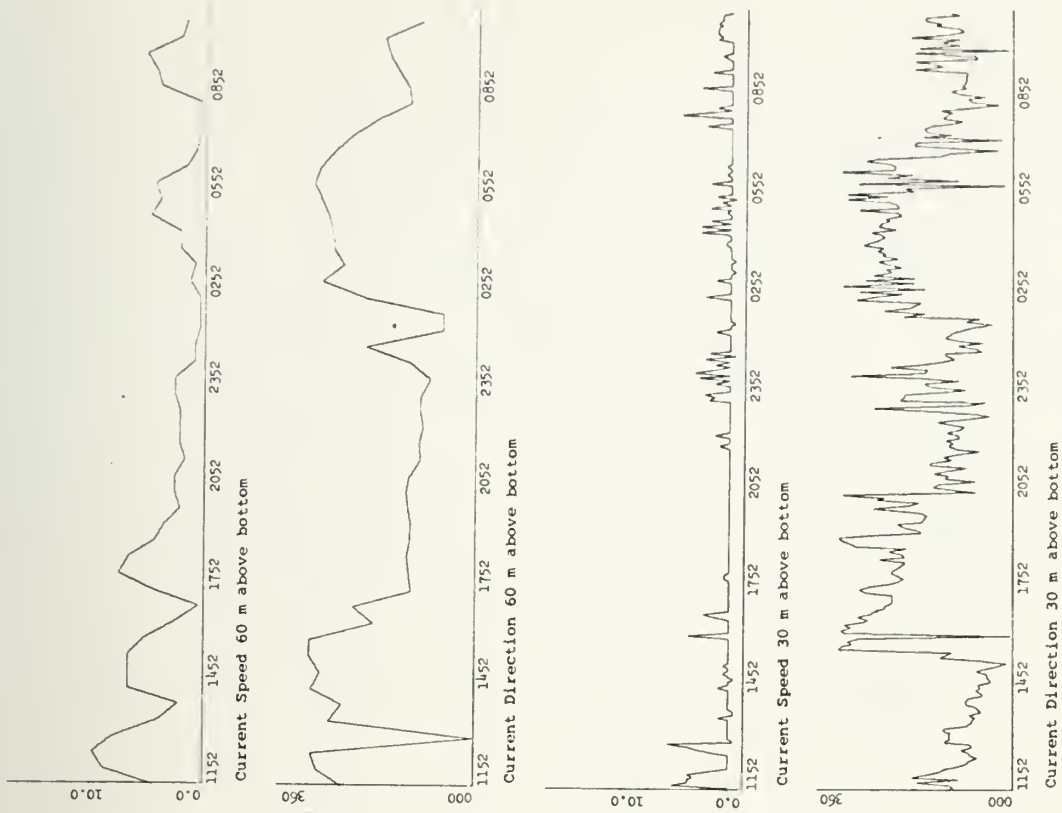


Fig. 22. Composite Drawings,  
5 Nov - 6 Nov



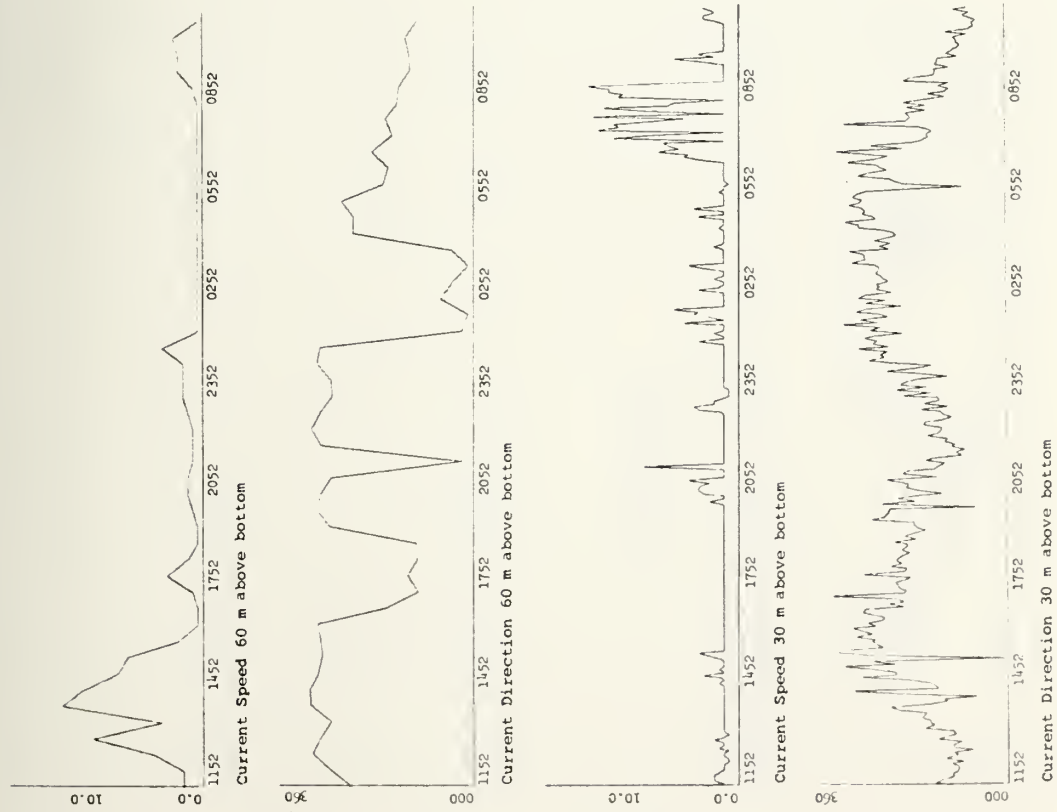


Fig. 23. Composite Drawings,  
6 Nov - 7 Nov

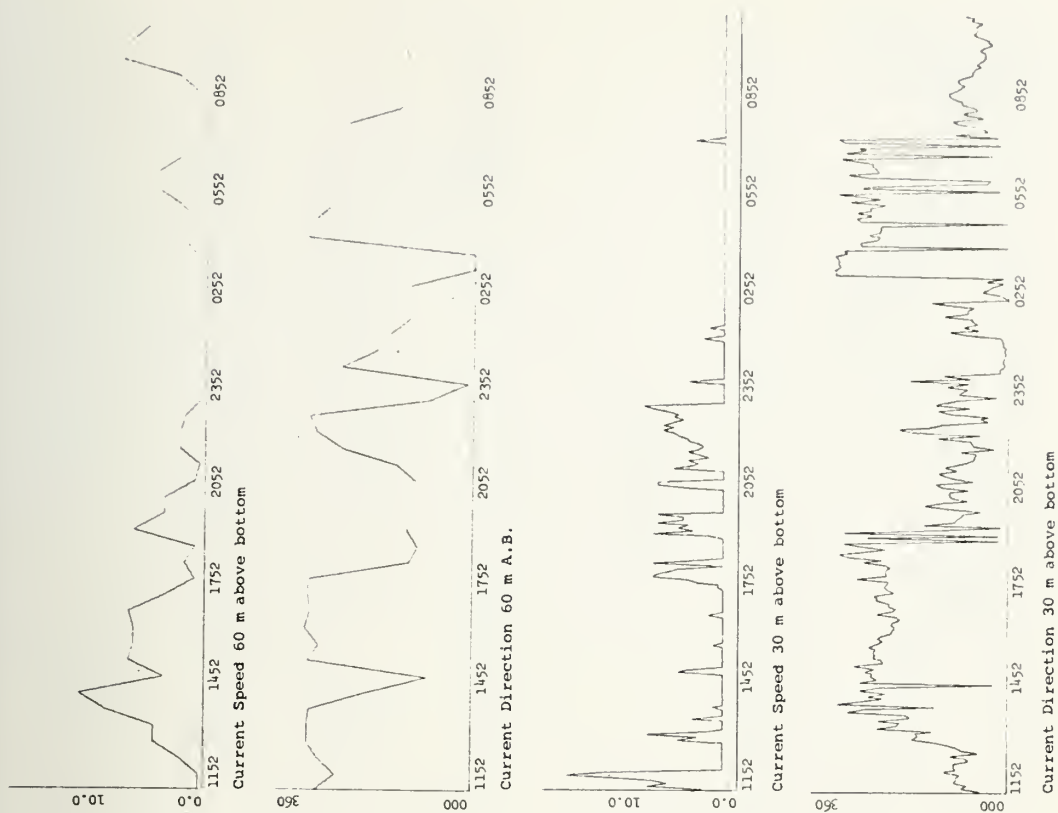


Fig. 24. Composite Drawings,  
7 Nov - 8 Nov



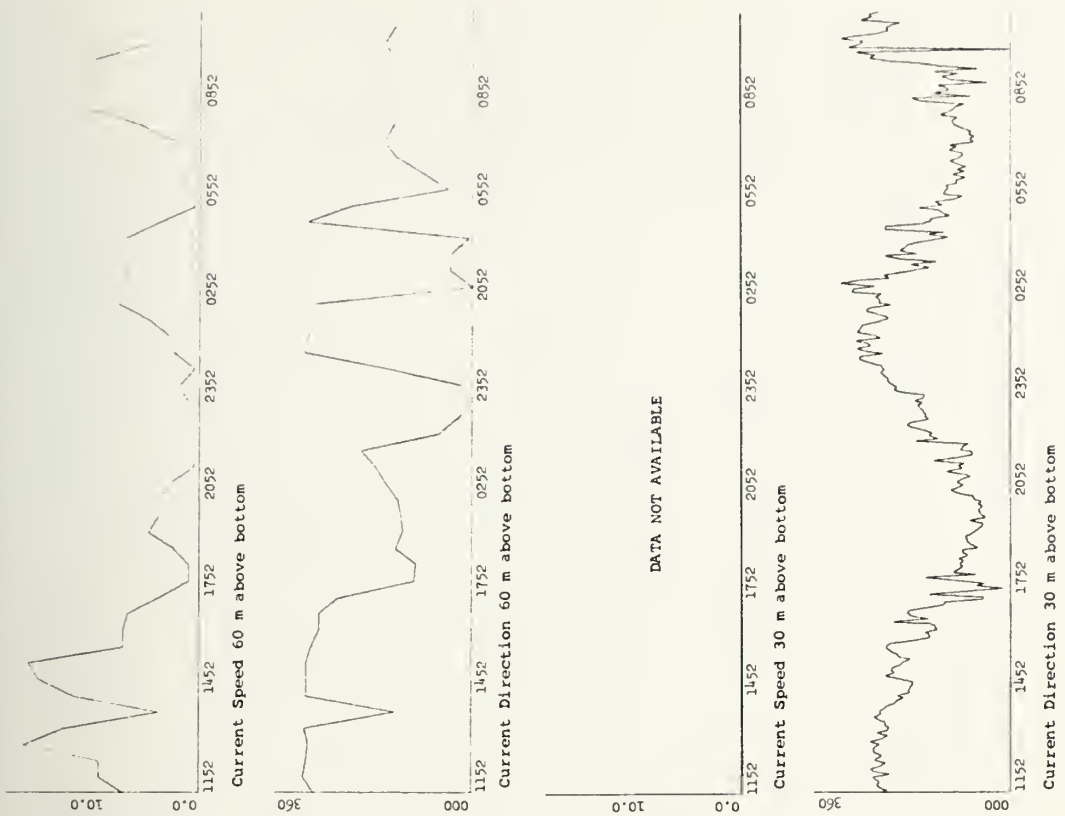


Fig. 25. Composite Drawings,  
8 Nov - 9 Nov

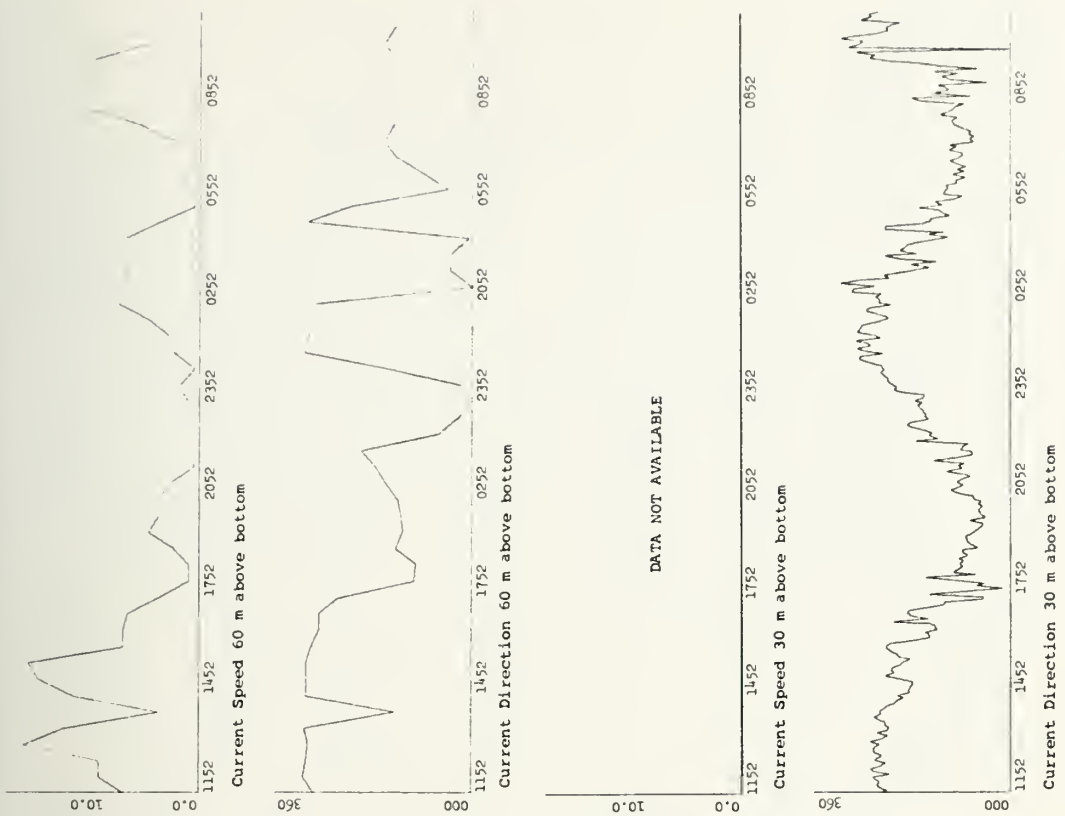


Fig. 26. Composite Drawings,  
9 Nov - 10 Nov





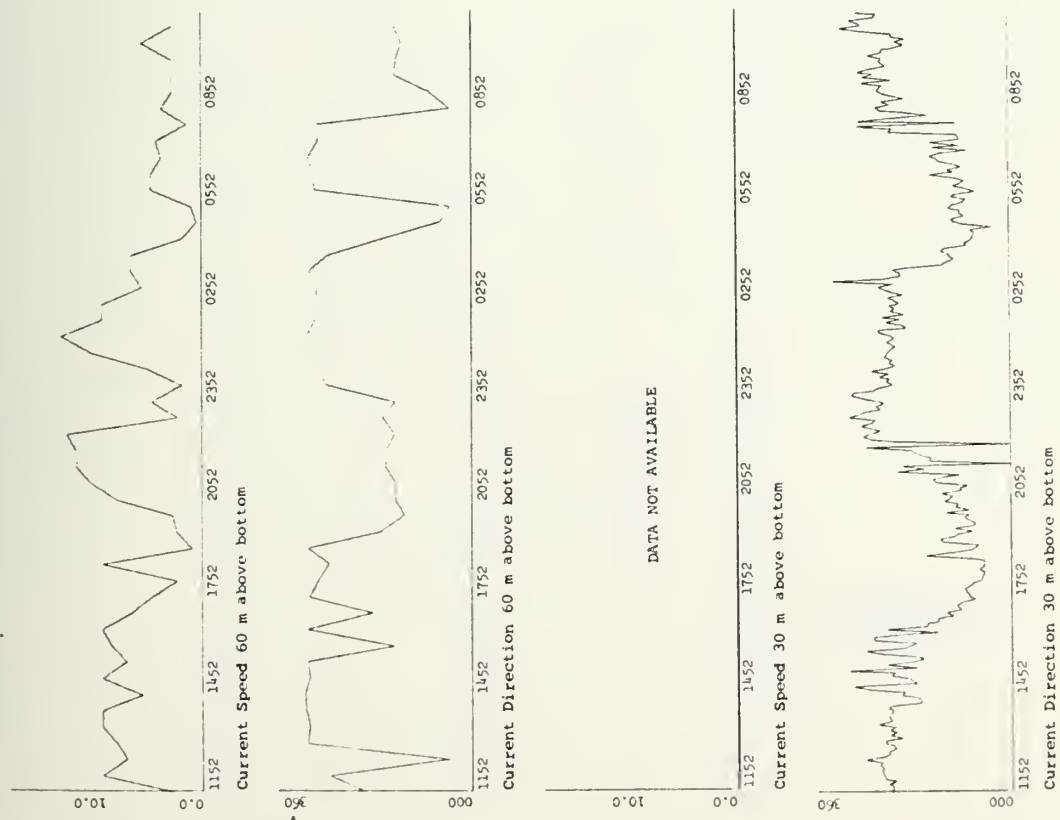


Fig. 27. Composite Drawing,  
10 Nov - 11 Nov

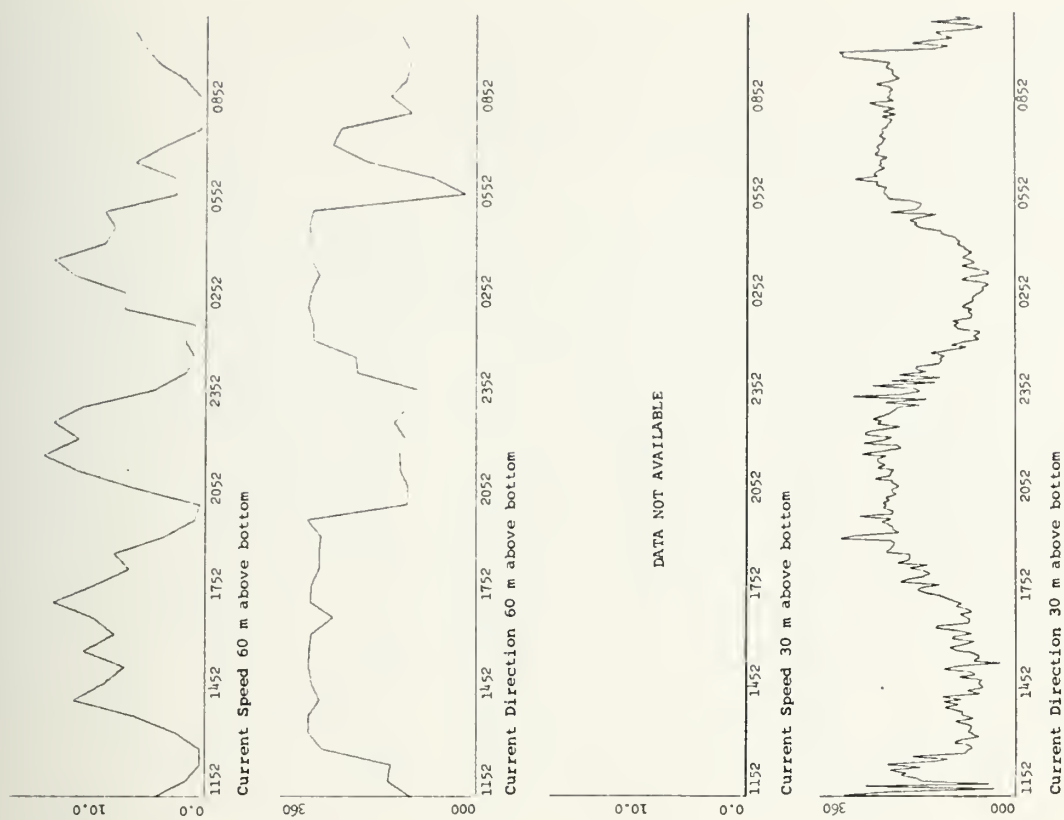
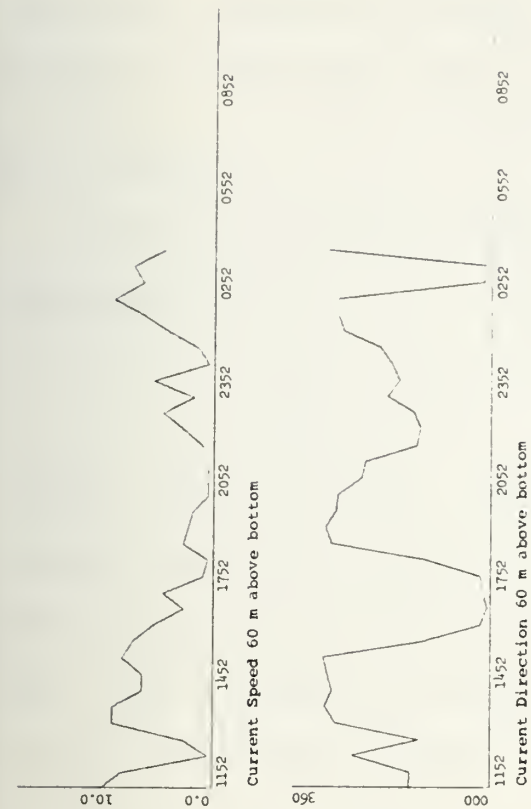
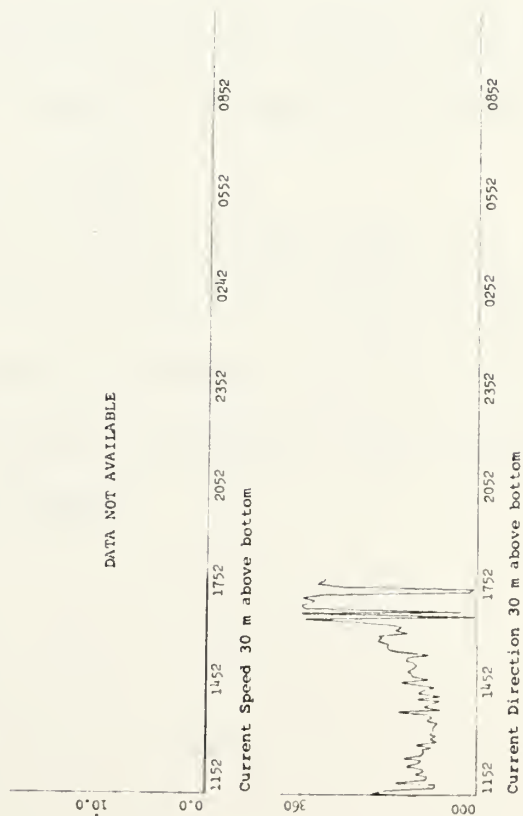


Fig. 28. Composite Drawing,  
11 Nov - 12 Nov





DATA NOT AVAILABLE



DATA NOT AVAILABLE

Fig. 29. Composite Drawings,  
12 Nov - 13 Nov



DATA NOT AVAILABLE

Current Speed 30 m above bottom

Current Direction 30 m above bottom

Fig. 30. Composite Drawings,  
13 Nov - 14 Nov



employed: values were picked off the strip chart by hand and points of cross-over were avoided.

#### D. ALIASING

The Hydro Products Model 502 current meter, with a 30-min sampling interval, has a cutoff frequency, defined by:

$$f_c = \frac{1}{2h}, \text{ where } h = \text{sampling interval,}$$

of one cycle per hour. Therefore, although useful for resolving tidally-generated fluctuations, this sampling rate is useless for defining frequencies higher than 1 cycle/hr. Furthermore, the lower frequencies will be contaminated by high frequencies if the latter are present in the signal before sampling.

#### E. HIGHER ORDER STATISTICS

Autospectra and cross-spectra were calculated for the two time series using BMD 02T, a computer program from the Health Sciences Computing Facility at UCLA.

A constant time interval of 30.0 min was used; 50 lags, equalling 7.2% of the data, were chosen to provide adequate resolution in the power spectral estimates, and all data were detrended to remove any frequency components whose periods were longer than the record length.



#### IV. DISCUSSION

The discussion which follows deals with the recorded data on two levels: (i) the apparent characteristics, which describe the general character of the current flow and are determined by examination of the various graphic presentations; (ii) the spectral characteristics, which describe the variability of the time series and the character of their periodic and irregular oscillations.

##### A. APPARENT CHARACTERISTICS

Very generally, the currents observed during the course of this investigation were similar in character to those observed and reported on by previous investigators. Current directions oscillated up and down or across the canyon and speeds (the scalar magnitude of current vectors) were variable with recorded maxima of the order of <sup>0.4 kn</sup> 20 cm/sec.

Table III shows a summary of the elementary statistics from both current meter records. The mean speed for each record was significantly lower than those reported by earlier investigators; speed variations, instead of oscillating smoothly, appeared as a series of peaks or spikes, particularly in the case of the record 30 m above-bottom (Fig. 15 through 24). The volume transport (in cubic meters/hour) calculated in program VECTOR DRAW (Appendix C) was also significantly lower than that reported by other investigators, and is particularly interesting in that the rate of flow





	30 m Above Bottom	60 m Above Bottom
Mean scalar speed	2.01 cm/sec	4.19 cm/sec
Mean up-canyon component	0.309 cm/sec	0.003 cm/sec
Mean cross-canyon component	0.131 cm/sec	0.978 cm/sec
Mean velocity	0.336 cm/sec	0.978 cm/sec
Maximum scalar speed	17.50 cm/sec	21.62 cm/sec
Maximum up-canyon component	6.36 cm/sec	9.56 cm/sec
Maximum cross-canyon component	8.67 cm/sec	18.01 cm/sec
$\sigma$ (scalar speeds)	1.41 cm/sec	3.95 cm/sec
$\sigma$ (up-canyon)	0.945 cm/sec	0.039 cm/sec
$\sigma$ (cross-canyon)	0.985 cm/sec	0.073 cm/sec
Vector mean direction	193.16 <sup>0</sup>	217.89 <sup>0</sup>
Volume transport/hr (per square meter)	12.08 m <sup>3</sup> /hr	36.97 m <sup>3</sup> /hr

TABLE III. Elementary Current Statistics



increases with distance above bottom. Although this is the condition commonly found in the open ocean, it is contrary to the results, presented by other investigators, of current studies in submarine canyons.

Current directions oscillated fairly smoothly with a discernible period of about 12 hr, with higher-frequency oscillations superimposed (Fig. 15 through 30). The frequencies of oscillation of the scalar speeds are sometimes doubled due to the rectification that is inherent with this type of plot. The direction histograms (Fig. 8a and 8b) show the characteristic bi-modal shape expected of a record from within the narrow confines of the canyon.

The canyon axis at the investigation site is oriented  $080^{\circ}$  -  $260^{\circ}$ . The dominant modes of the direction histogram from the 30 m above-bottom record (Fig. 8a) indicate that the flow is predominantly along the canyon axis at that depth. The direction histogram from the 60 m above-bottom record (Fig. 8b), however, shows dominant modes perpendicular to the canyon axis indicating that the flow has a strong cross-canyon component. This is confirmed by the scatter diagram for this level (Fig. 14). This cross-canyon flow obviously cannot continue for any great distance because of the canyon walls; local direction deviations due to topography must therefore occur. The causes of this cross-canyon flow are speculative. As mentioned earlier, Shepard, Marshall and McLoughlin [1974a] have suggested a relation between the occurrence of cross-canyon winds and cross-canyon current surges, and noted a



repetition cycle that is apparently tidally influenced. In deep canyons the cross-canyon flow may be caused by local topographic effects, or by semi-permanent eddy structures along the canyon walls. It may also be due to intrusion into the canyon of motions along the continental slope.

The direction of net transport can be inferred from the progressive vector diagrams (Fig. 9 and 10) by noting the apparent net direction of particle movement. This direction is  $220^{\circ}$  for the record 30 m above bottom and  $330^{\circ}$  for the record 60 m above bottom. These diagrams are drawn to the same length scale so that relative flows may be seen. The expanded diagrams (Fig. 11 and 12) fill the printing frame and more clearly show the details of the flow, but have different scales. In these diagrams successive 24-hr periods are marked with an "X".

The composite drawings of current direction versus time (Fig. 15 through 30) clearly show oscillatory changes of direction with a dominant period of approximately 12 hr. This characteristic is particularly apparent in the record 30 m above bottom, due to the higher sampling rate employed there, but can also be seen in the record 60 m above bottom. There is a phase difference between the two levels of about 4 hr. It is interesting that the 4-hr time period corresponds to  $90^{\circ}$  of tidal rotation. It is not clear, however, that the observed  $90^{\circ}$  (approximate) angular displacement between the two levels has its cause in this factor. The vertical coherence of these oscillations will be discussed in the section on spectral characteristics.



Speed oscillations are much less clearly defined in both records, but peaks tend to occur every 5 to 6 hr, which is characteristic of a reversing current with a 10- to 12-hr period. A relationship between peak speeds and direction is not evident in these graphs, but may clearly be seen in the graphs of up-canyon and cross-canyon components versus time (Fig. 31 and 32).

## B. SPECTRAL CHARACTERISTICS

Power spectral estimates of the two time series were generated to identify the frequencies which contribute to the overall variability of the series. Spectral estimates are presented in a linear plot against frequency to avoid the area distortion of the common logarithmic presentation. Power spectra were computed for (i) up-canyon velocity 60 m above bottom (Fig. 33); (ii) cross-canyon velocity 60 m above bottom (Fig. 34); (iii) up-canyon velocity 30 m above bottom (Fig. 35); (iv) cross-canyon velocity 30 m above bottom (Fig. 36). Aperiodic fluctuations and surges, possibly due to solitary internal waves or eddies from the California Current, are reflected in the very low frequency portions of the spectra.

The phase, coherence, and cross-spectral estimates were computed between: (i) 60 m up-canyon velocity and 30 m up-canyon velocity; (ii) 60 m cross-canyon velocity and 30 m cross-canyon velocity; (iii) 60 m cross-canyon velocity and 30 m up-canyon velocity.





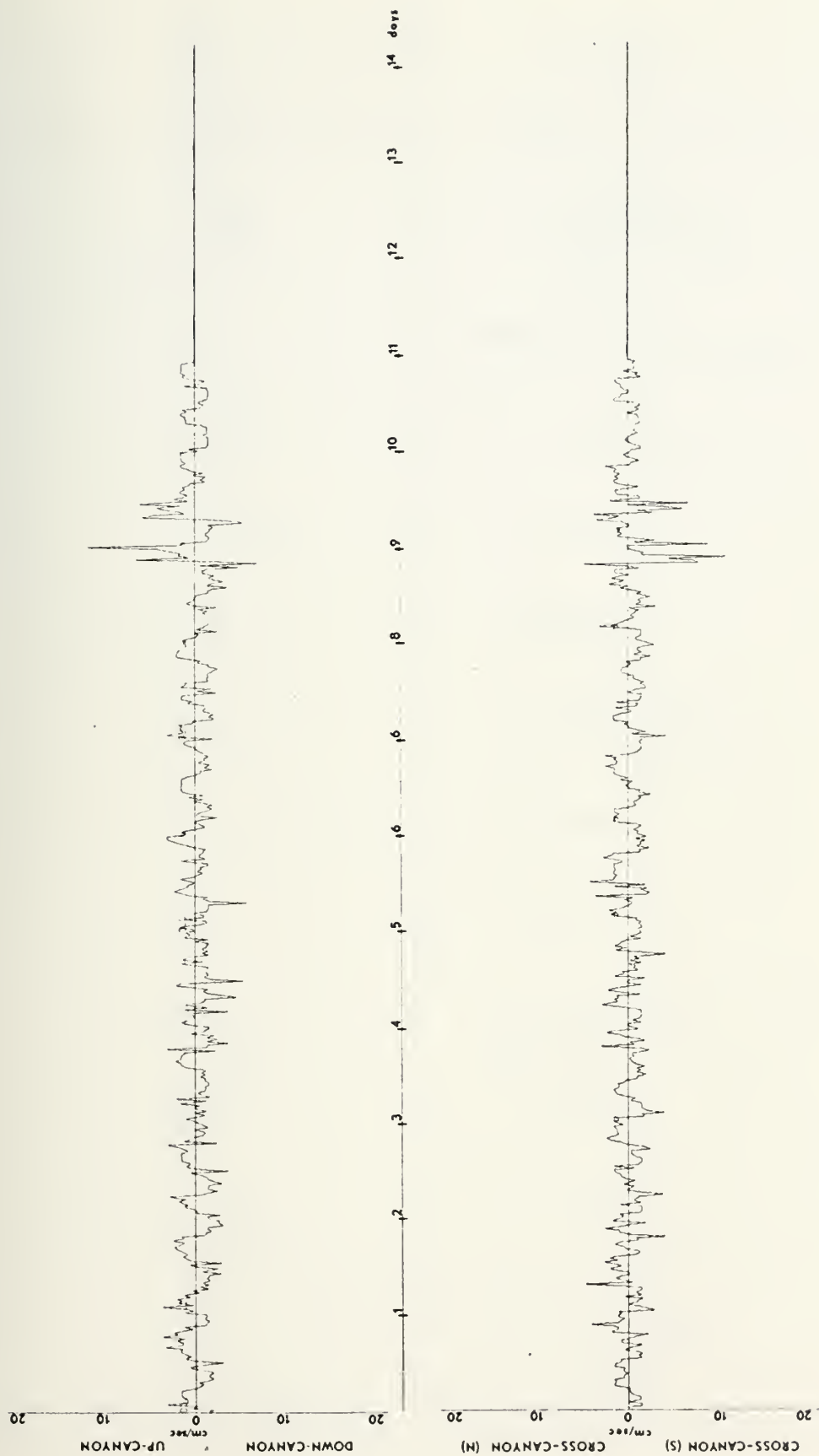


Fig. 31. Directional Components versus Time, 30 m above bottom.



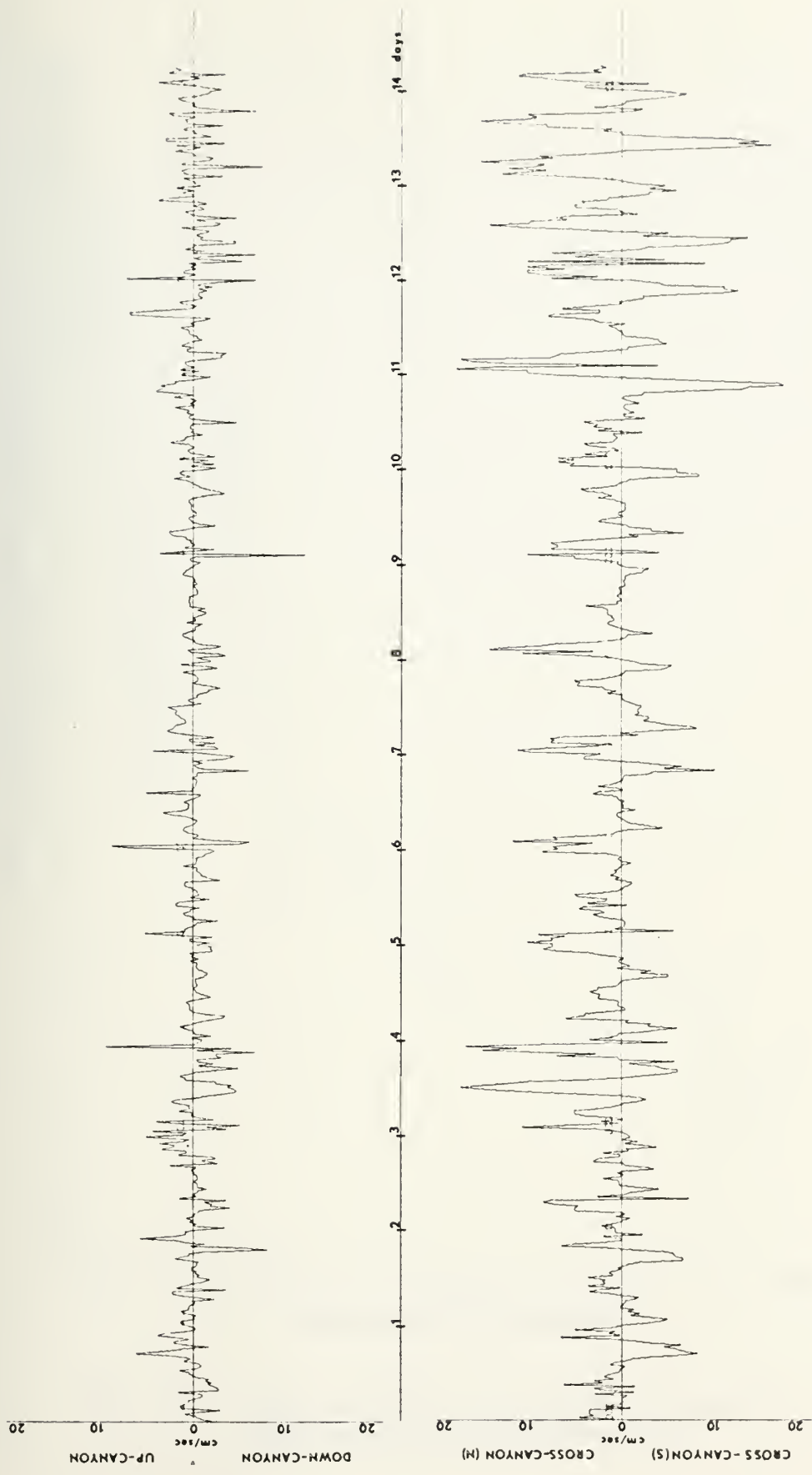


Fig. 32. Directional Components versus Time, 60 m above bottom.



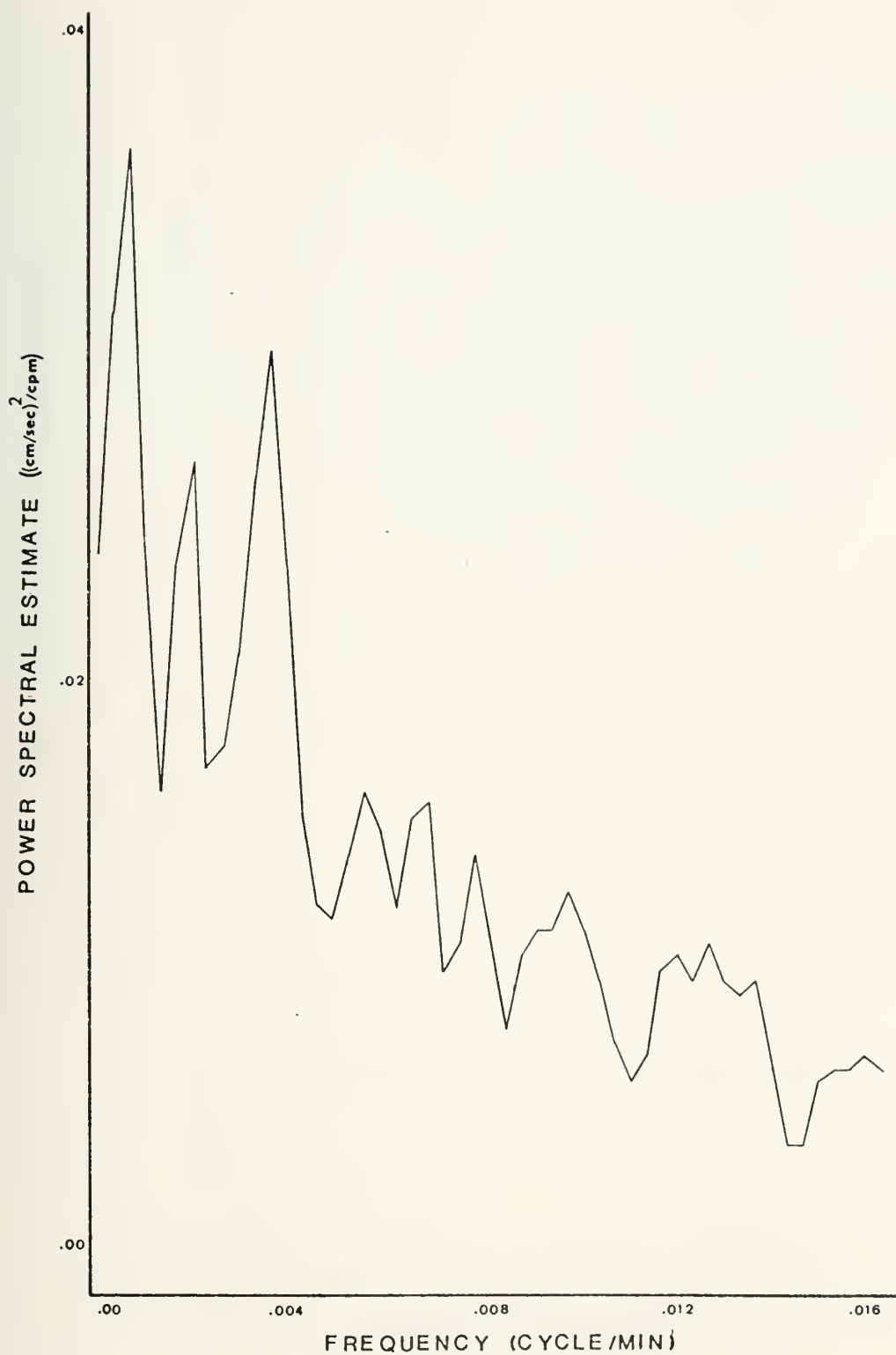


Fig. 33. Power Spectral Estimate, Up-Canyon Component 60 m above bottom



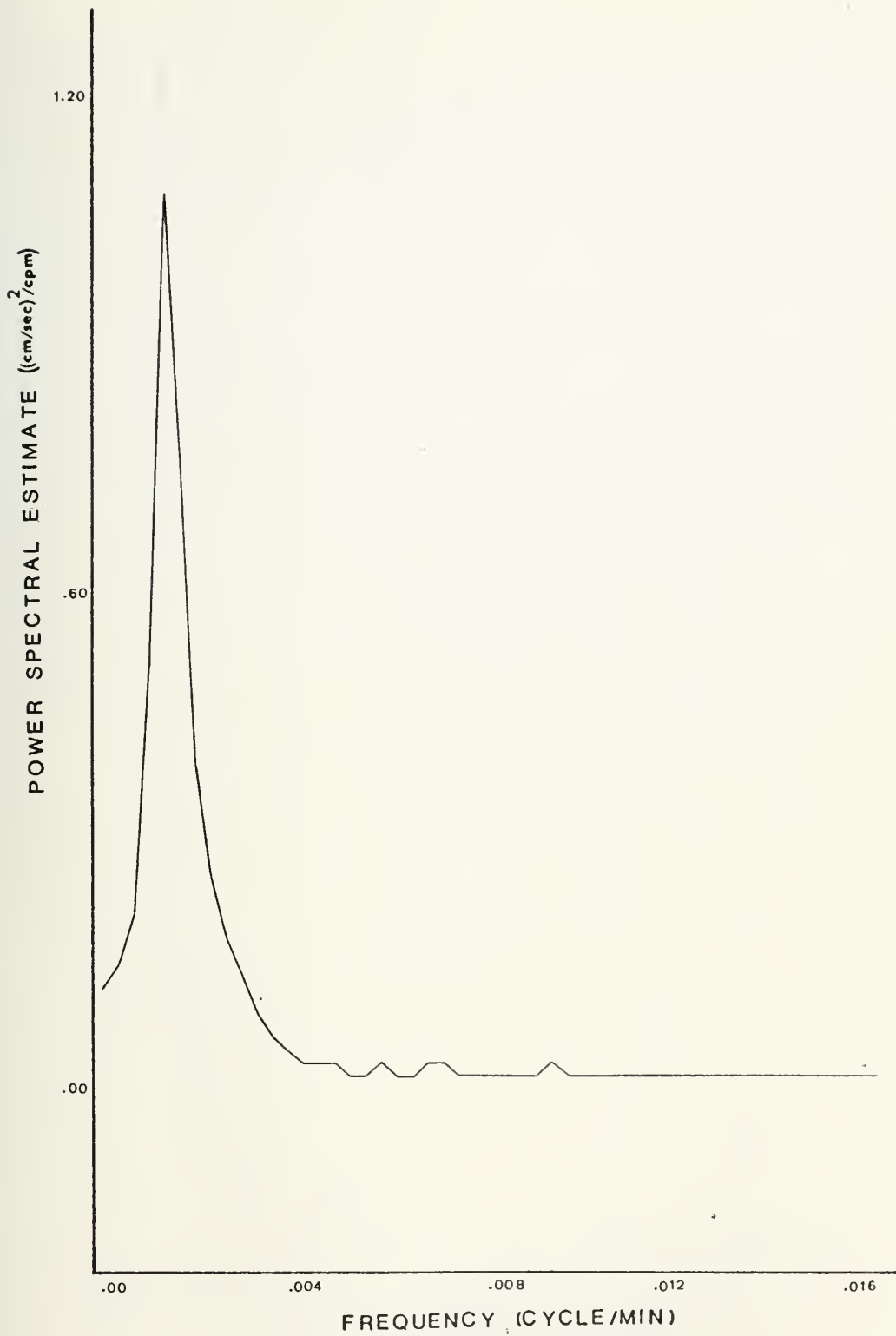


Fig. 34. Power Spectral Estimate, Cross-Canyon Component 60 m above bottom





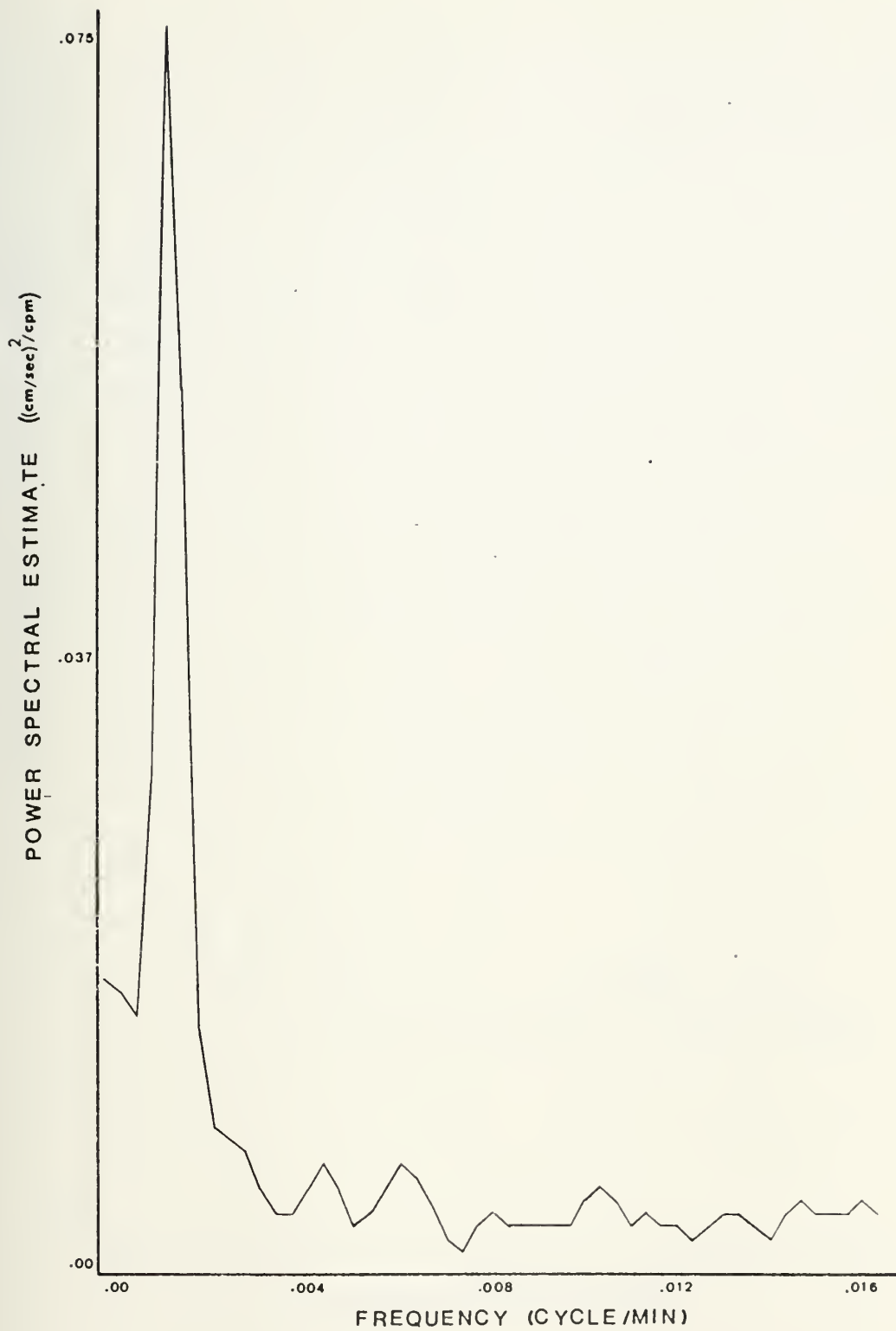


Fig. 35. Power Spectral Estimate, Up-Canyon  
Component 30 m above bottom



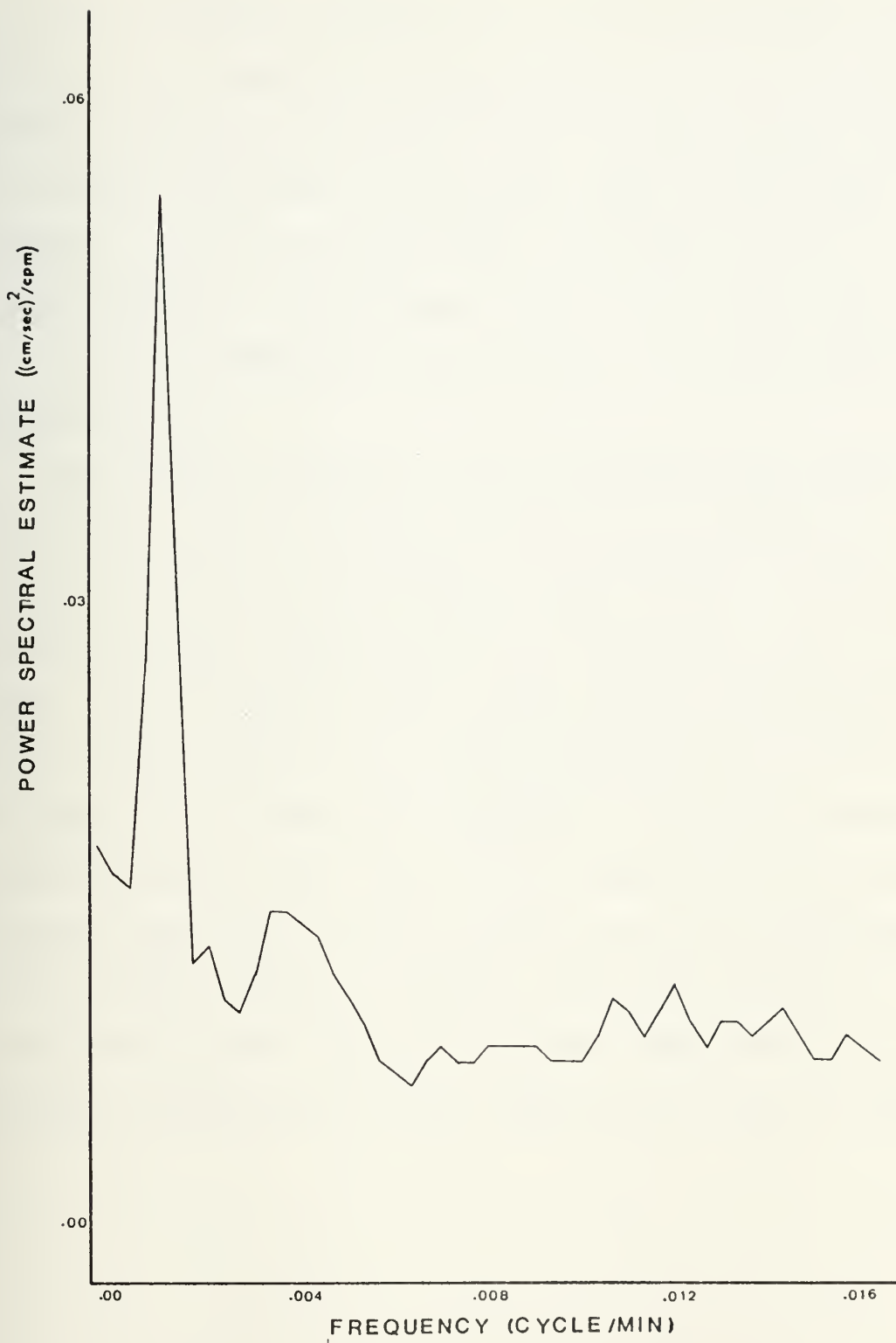


Fig. 36. Power Spectral Estimate, Cross-Canyon Component 30 m above bottom



Power spectral estimates for the 30 m up-canyon and 60 m cross-canyon components are very clean, each with a dominant peak at a period of 12.4 hr. The 30 m cross-canyon spectrum also shows this peak, but has more noise in the higher frequencies. The 12.4-hr peak does not appear in the 60 m up-canyon spectrum; the highest energy in this spectrum, which is far noisier than the others, occurs at a period of approximately 24 hrs.

The frequency content of the component pairs previously listed was clearly visible in the cross-covariances. Again, the 12.4-hr period was prominent, particularly in the up-canyon and cross-canyon component pairs. Coherences were low and noisy. The cross-covariance of the 30 m up-canyon and 60 m cross-canyon records also showed the prominent 12.4-hr period for most of the record, but values of the cross-covariance function hovered near zero for one segment of the record. Although there are several possible causes for this phenomenon, such as phase changes or effects indirectly related to a change from even to uneven tides, no obvious solution to the problem presents itself except to use longer time series in the future.



## V. CONCLUSIONS

The directional trends recorded, particularly the very strong cross-canyon component of the 60 m above-bottom record, further support the contention of Shepard and Marshall [1973b] that there may be a level above the bottom beyond which current direction is reversed. The cross-canyon flow may also be due to the intrusion of currents along the continental slope into the canyon. Since the coherence values are lower than might be expected from two current meters separated by only 30 m, it is possible that the upper instrument was in the vicinity of a near-bottom boundary layer, perhaps caused by a moving suspension of sediments in the bottom layer. It is also possible that the coherence has degenerated from the effects of noise.

Previous investigators have reported decreasing current speeds with distance above the bottom. The higher speeds and volume transport values obtained from the instrument 60 m above the bottom were therefore unexpected, but not unreasonable. One would expect near-bottom current speeds to be lower because of bottom friction. Continuous down-slope sediment transport could be a factor contributing to higher current speeds very near the bottom. If, however, the 60 m currents are associated with along-slope currents rather than down-canyon flow, the higher speeds are not surprising.

The 12.4-hr oscillations revealed in the spectral analysis are undoubtedly due to tides or tidally influenced phenomena.





The cause or causes of the shorter period oscillations, however, remain unidentified. These shorter periods of oscillation are of the proper order of magnitude for internal waves and the differing amounts of energy occurring in the higher frequency portions of the up-canyon spectral estimates could be explained by the diverse mode patterns associated with internal waves.

Current flow 30 m above the bottom is predominantly along the canyon axis and appears to be tidally-driven. This current is probably related to a steady down-canyon transport of suspended sediment. At 60 m above the bottom the current is a well established cross-canyon flow that is only slightly perturbed by up- and down-canyon tidal oscillations. This can be seen in the progressive vector diagram (Fig. 10). Coherence between the two current meter records is low and noise-like, and the two signals are essentially not correlated.

Further investigations to define the complex nature of current flow in submarine canyons are clearly warranted. Verification of the above hypotheses could be accomplished by a series of multiple instrument/multiple array investigations with current meters deployed at 3 m, 30 m, 60 m, and 90 m above the bottom and arrays spaced at 4 km intervals, approximately one-fourth the wavelength of an internal wave, along the canyon axis. The arrays should be deployed for at least 30 days to include a complete tidal cycle.



# APPENDIX A: Program SUBMARINE CANYON

PROGRAM SUBMARINE CANYON PROVIDES ELEMENTARY STATISTICS FOR  
TIME SERIES OF CURRENT SPEED, CURRENT DIRECTION, AND  
TEMPERATURE. MEANS ARE COMPUTED HOURLY, DAILY, AND FOR THE  
ENTIRE SERIES. A HISTOGRAM IS PROVIDED DAILY AND FOR EACH  
SERIES. VARIANCES AND STANDARD DEVIATIONS ARE COMPUTED FOR  
EACH SERIES.

DIMENSION DATE(3), DATO(3), TIME(5000), T(5000), S(5000), D(5000),  
I M(5000), ASI(8), MDI(8)  
REAL LABEL /4H

IND = NUMBER OF DATA SETS

IND = 1

DO 250 I I I=1, IND  
CLOCK = I TIME(0)\*0.01

CONTROL CARD INPUT:

READ (5,280) NN,NO,NT,NA,NH,NP,PN,NW,PW,ICOR,IMO,DATE,DATO,INKTS

ENTER WITH: NN=NUMBER OF DATA POINTS. CALL DRAW MUST BE  
ADJUSTED TO TOTAL OF NN POINTS (I4).

NO=DAY OF FIRST OBSERVATION (I2).

NT=TIME OF FIRST OBSERVATION (I4).

NA=LARGEST NT LESS THAN 2400 (I4).

NH=HOUR FRACTION (IN MINUTES) OF FIRST

OBSERVATION (I2).

NP=LATITUDE DEGREES (I2).

PN=LATITUDE MINUTES (F6.2).

NW=LONGITUDE DEGREES (I3).

PW=LONGITUDE MINUTES (F6.2).

ICOR=DIRECTION CORRECTION FOR MAGNETIC VARIATION (I3)

IMO=LAST DAY OF MONTH (I3).

DATE=MONTH OF OBSERVATION (3A4).

DATO=DATE PLUS ONE MONTH (3A4).

INKNTS=1 CONVERTS DATA IN KNOTS TO CM/SEC.

DEL = SAMPLING INTERVAL IN MINUTES.

DEL = 5.0

SI PLUS 1.0 = NUMBER OF SAMPLES PER HOUR

SI = ((60.0/DEL)-1.0)

TIME(1) = 0.



```

C      NODRW = 0
C      NODRW = 1 IF NO GRAPHS ARE DESIRED.
C      L = 0
C      NZ = 0
C      IDAY = 1
C      WRITE (6,290) NP,PN,NW,PW,NO,NT,DATE
C      WRITE (6,300)
C      WRITE (6,310) NO,NT,DATE
C      INPUT TEMPERATURE, SPEED, AND DIRECTION TIME SERIES.
C
C      DO 100 I=1,NN,5
C      READ (5,320,END=120) (T(I+K-1),S(I+K-1),M(I+K-1),K=1,5)
C      100 CONTINUE
C
C      CONVERT TO CM/SEC IF INPUT IS IN KNOTS (INKTS=1).
C      IF (INKTS.NE.1) GO TO 120
C
C      DO 110 I=1,NN
C      110 S(I) = S(I)*51.479
C      120 CONTINUE
C
C      COMPUTE HOURLY AND SERIES MEANS.
C      N1 IS A COUNTER FOR ACCUMULATING AVERAGES BY 8'S.
C      N1 = 0
C      DO 220 I=1,NN
C      ADJUST DIRECTION IF REQUIRED.
C      M(I) = M(I)+ICOR
C      IF (M(I)-0.) 130,140,140
C      130 M(I) = M(I)+360
C      140 CONTINUE
C      IF (M(I).LT.360) GO TO 150
C      150 M(I) = M(I)-360
C      CONTINUE
C      N = I
C      IF (T(I).EQ.1.) GO TO 220
C      WRITE (6,330) TIME(I),T(I),S(I),M(I),I
C      IF (L.LT.SI) GO TO 210

```



```

C C C C C
SI PLUS 1.0 IS THE NUMBER OF SAMPLES PER HOUR. THIS
FIGURE IS INTERNALLY ADJUSTED FOR DIFFERENT SAMPLING
INTERVALS IN ORDER TO COMPUTE HOURLY MEANS.
NT = NT+100
IF (NT.LE.NA) GO TO 160
NT = 0000+NH
NJ = ND+1
IMN = I-NZ
PROGRAM COMPUTES STATISTICS AT END OF EACH DAY.
CALL DAY (T,S,M,IMN,I,1,DTAV,DSAV,DDAV)
IDDAV = IFIX(DDAV)
WRITE (6,260) IDAY,DTAV,DSAV,IDDAV
IDAY = IDAY+1
NZ = 0
IF MONTH CHANGES, REPLACE THE DATE.
160 IF (NO.LE.IMO) GO TO 180
NO = 1
DO 170 J=1,3
170 DATE(J) = DATO(J)
180 CONTINUE
HR = TIME(I)/60
IML = I-L
CALL SUBROUTINES FOR HOURLY MEANS.
NI = NI+1
CALL MEAN (T,IML,I,AT)
CALL MEAN (S,IML,I,AS)
ASI(NI) = AS
CALL MEAN (M,IML,I,S,AVG)
MD = IFIX(AVG)
IF (MD.GE.0) GO TO 190
MD = 360+MD
CONTINUE
190 MD1(NI) = MD
SPEED AND DIRECTION AVERAGES ACCUMULATED BY 8'S FOR PUNCHED CARD
INPUT INTO PROGRAM VECTOR DRAW.
IF (NI.LT.8) GO TO 200

```





1440  
1450  
1460  
1470  
1480  
1490  
1500  
1510  
1520  
1530  
1540  
1550  
1560  
1570  
1580  
1590  
1600  
1610  
1620  
1630  
1640  
1650  
1660  
1670  
1680  
1690  
1700  
1710  
1720  
1730  
1740  
1750  
1760  
1770  
1780  
1790  
1800  
1810  
1820  
1830  
1840  
1850  
1860  
1870  
1880  
1890  
1900  
1910

```

C      N1 = 0
C      WRITE (7,270) (AS1(K),MD1(K),K=1,8)
C      CONTINUE
C
C      WRITE OUT HOURLY MEANS.
C
C      WRITE (6,340) ND,NT,DATE,HR,AT,AS,MD
C      L = -1
C      TIME(I+1) = TIME(I)+DEL
C      NZ = NZ+1
C      L = L+1
C      CONTINUE
C
C      WRITE (7,270) (AS1(K),MD1(K),K=1,8)
C      N = NN
C
C      COMPUTE THE TIME SERIES MEANS.
C
C      CALL MEAN (T,1,N,TAT)
C      CALL MEAN (S,1,N,TAS)
C      CALL MEAN (M,1,N,S,AVG)
C      MMD = IFIX(AVG)
C      IF (MMD.GE.0) GO TO 230
C      MMD = 360+MMD
C      CONTINUE
C      WRITE (6,350) TAT,TAS,MMD
C
C      DO 240 I=1,N
C      D(I) = FLOAT(M(I))
C      CONTINUE
C
C      CALL HISTO SUBROUTINE FOR TIME SERIES HISTOGRAM.
C
C      CALL HISTO (0.,10.,20,T,NN,1,NOODRW)
C      CALL HISTO (0.,75.,15,S,NN,1,NOODRW)
C      CALL HISTO (0.,360.,36,D,NN,1,NOODRW)
C
C      CALL SUBROUTINE POWER FOR RMS, VARIANCE, AND STANDARD DEVIATIONS.
C
C      CALL POWER (DEL,NN,T,S,D,100)
C      CLOCK = ITIME(0)*0.01-CLOCK
C      WRITE (6,360) CLOCK
C      CONTINUE
C
C      STOP
C
C

```



```

260 FORMAT (5X,'DAY ',I2,' STATISTICS:  AVGDAYTEMP=',F6.2,3X,
1  'AVGDAYSPEED=',F5.2,3X,'AVGDAYDIR=',I4,/)
270 FORMAT (8(F5.2,I4))
280 FORMAT (I4,I2,I4,I2,I4,I2,F6.2,I3,F6.2,2I3,3A4,3A4,I2)
290 FORMAT (I4,I2,I4,I2,I4,I2,F6.2,I3,F6.2,2I3,3A4,3A4,I2)
1 //I,5X,'METER POSITION: ',I2,F6.2,' N ',I3,F6.2,' W ',
2 //,5X,'ZERO TIME: ',I2,I4,'(LOCAL)',3A4,
3 //,5X,'TIME IN MINUTES: ',
4 //,5X,'TEMPERATURE IN DEGREES CENTIGRADE ',SECOND',
5 //,5X,'CURRENT SPEED IN CENTIMETERS PER SECOND',
6 //,5X,'CURRENT DIRECTION IN DEGREES TRUE',//)
300 FORMAT (I5X,'TIME',I0X,'TEMPERATURE',6X,'CURRENT SPEED',4X,
1  'CURRENT DIRECTION')
310 FORMAT (I4X,I2,I4,3A4)
320 FORMAT (5(F5.1,F5.2,I4))
330 FORMAT (I0X,F10.2,I3X,F4.1,I5X,F5.2,14X,I3,5X,I5,5X,I5)
340 FORMAT (I4X,I3,I4,3A4,2X,F5.1,'HRS',4X,'MEAN TEMP:',
1  F6.2,4X,'MEAN SPEED:',F5.2,2X,'MEAN DIR:',I3,/)
350 FORMAT (I4X,I1X,'MEANS FOR THIS RECORD:  TEMP:',F6.2,2X,'SPEED:',
1  F5.2,2X,'DIRECTION:',I3)
360 FORMAT (//,T80,'ELAPSED COMPUTING TIME=',F15.7,'SECONDS')
      END

```

```

SUBROUTINE MEAN (A,J,M,AVG)
C
C SUBROUTINE MEAN COMPUTES THE ARITHMETIC MEAN OF ANY
C INPUT PARAMETER.
C
      DIMENSION A(5000)
      AVG = 0.0
      SUM = 0.0
      KK = M-J+1
      FKK = FLOAT(KK)
C
      DO 100 K=J,M
100 SUM = SUM+A(K)
C
      AVG = SUM/FKK
      RETURN
      END

```

```

SUBROUTINE MEAND (LL,J,M,S,AVG)
C
C SUBROUTINE MEAND COMPUTES THE MEANS OF DIRECTION INPUTS AS COMPASS

```



```

C HEADINGS BY SUMMING SINES AND COSINES; CONVERT TO VECTOR WITH
C SPEED THEN NORMALIZE AND FIND THE ARCTANGENT. THIS PROCEDURE
C IS NECESSARY TO CIRCUMVENT THE 000 TO 360 DISCONTINUITY.
C
C DIMENSION LL(5000), S(5000)
C SUM1 = 0.0
C SUM2 = 0.0
C
C DO 110 K=J,M
C AK = LL(K)*0.01745329
C IML = M-J+1
C IF (S(K).GT.0.0) GO TO 100
C
C SPEED NOT AVAILABLE. READ FROM DATA CARD AS S(K)=0.0.
C INSERT FALSE VALUE TO ELIMINATE DIVISION BY ZERO.
C
C S(K) = 0.001
C 100 CONTINUE
C SUM1 = SUM1+S(K)*SIN(AK)
C SUM2 = SUM2+S(K)*COS(AK)
C 110 CONTINUE
C
C U = SUM1/FLOAT(IML)
C V = SUM2/FLOAT(IML)
C AVG = ATAN2(U,V)
C AVG = AVG/.01745329
C RETURN
C END
C
C SUBROUTINE HISTO (A,Z,K,X,L,M,NODRW)
C
C SUBROUTINE HISTO OBTAINS HISTOGRAM, PERCENT OF DATA PER INTERVAL,
C PROBABILITY DENSITY, AND PROBABILITY DISTRIBUTION.
C ENTER WITH:
C A=LOWER BOUND
C Z=UPPER BOUND
C K=NUMBER OF INTERVALS (MAX=50)
C X=VARIABLE NAME
C L=NUMBER OF VARIABLES (MAX=3000)
C NODRW=1 IF GRAPH NOT DESIRED
C
C DIMENSION N(5000), X(5000), P(55), PP(55), D(55), PD(55), B(5000)
C REAL #8 ITITLA(12)
C REAL LABEL/4H /
C IF (NODRW.EQ.1) GO TO 100
C READ (5,250) (ITITLA(I),I=1,12)

```



EACH TITLE (THERE ARE THREE) CONSISTS OF TWO CARDS WITH NO MORE  
THAN 48 CHARACTERS EACH.

```

C
C
C
100 CONTINUE
WRITE (6,220)
LL = 0
C = (Z-A)/FLOAT(K)
D(I) = A
KP1 = K+1
KP2 = K+2
C
DO 110 I=2,KP2
IM1 = I-1
110 D(I) = A+IM1*C
C
SUMP = 0.0
C
DO 120 I=1,KP2
120 B(I) = 0
C
LLL = M+L
C
DO 160 J=M,LLL
C
DO 150 I=1,KP2
IP1 = I+1
IF (X(J).LT.D(I)) GO TO 150
IF (X(J).GE.D(I)) GO TO 130
130 IF (X(J).LT.D(IP1)) GO TO 140
GO TO 150
140 B(I) = B(I)+1
LL = LL+1
IF (X(J).LE.Z) GO TO 150
LL = LL-1
150 CONTINUE
C
160 CONTINUE
C
C
DO 170 I=1,KP2
170 P(I) = B(I)/FLOAT(LL)
C
C
DO 180 I=1,KP2
180 PP(I) = P(I)/C
C
C
DO 190 I=1,KP2

```









```

C      100 SUM3 = SUM3+Z(I)
C      XBAR = SUM1/N
C      YBAR = SUM2/N
C      ZBAR = SUM3/N
C      WRITE (6,150) XBAR,YBAR,ZBAR
C
C      TRANSFORMATION TO ZERO MEAN VALUE
C
C      DO 110 I=1,N
C      XM(I) = X(I)-XBAR
C      CONTINUE
C      110
C      CALL MEAN (XM,1,N,AVG)
C      WRITE (6,160) AVG
C
C      DO 120 I=1,N
C      YM(I) = Y(I)-YBAR
C      CONTINUE
C      120
C      CALL MEAN (YM,1,N,AVG)
C      WRITE (6,160) AVG
C
C      DO 130 I=1,N
C      ZM(I) = Z(I)-ZBAR
C      CONTINUE
C      130
C      CALL MEAN (ZM,1,N,AVG)
C      WRITE (6,160) AVG
C
C      CALCULATION OF THE MEAN SQUARE VALUE
C
C      SUM1 = 0.0
C      SUM2 = 0.0
C      SUM3 = 0.0
C
C      DO 140 I=1,N
C      SUM1 = SUM1+(X(I)-XBAR)**2
C      SUM2 = SUM2+(Y(I)-YBAR)**2
C      SUM3 = SUM3+(Z(I)-ZBAR)**2
C      CONTINUE
C      140
C      XMS = SUM1/N
C      YMS = SUM2/N
C      ZMS = SUM3/N
C      WRITE (6,170) XMS,YMS,ZMS
C

```



# CALCULATION OF THE STANDARD DEVIATION

```

C
C
XTEMP = SUM1/(N-1)
YTEMP = SUM2/(N-1)
ZTEMP = SUM3/(N-1)
SX = SQR(XTEMP)
YX = SQR(YTEMP)
ZX = SQR(ZTEMP)
WRITE(6,180) SX,YX,ZX
RETURN
C
150 FORMAT (T10,'SAMPLE MEANS:',/,T35,'XBAR= ',F10.3,/,T35,'YBAR= ',
1,F10.3,/,T35,'ZBAR= ',F10.3,///)
160 FORMAT (T40,F30.10)
170 FORMAT (T10,'MEAN SQUARE VALUES:',/,T35,'XMSQ= ',F10.3,/,T35,
1,'YMSQ= ',F10.3,/,T35,'ZMSQ= ',F10.3,///)
180 FORMAT (T10,'STANDARD DEVIATIONS:',/,T35,'XSTDDEV= ',F10.5,/,T35
1,'YSTDDEV= ',F10.5,/,T35,'ZSTDDEV= ',F10.5,///)
END

```

```

SUBROUTINE DAY (T,S,M,J,K,NODRW,DTAV,DSAV,DDAV)
SUBROUTINE DAY UTILIZES PREVIOUS SUBROUTINES TO OBTAIN
DAILY STATISTICS.

```

```

DIMENSION DH(5000), T(5000), S(5000), M(5000)

```

```

ENTER WITH: T=TEMPERATURE SERIES

```

```

S=SPEED SERIES

```

```

M=DIRECTION SERIES

```

```

J=DAY START OBSERVATION NUMBER

```

```

K=TOTAL OBSERVATIONS IN THE SERIES

```

```

NODRW=1 IF GRAPH NOT DESIRED

```

```

CALL MEAN (T,J,K,DTAV)
CALL MEAN (S,J,K,DSAV)
CALL MEAND (M,J,K,S,DDAV)
IF (DDAV.GE.0) GO TO 100
DDAV = DDAV+360
CONTINUE

```

```

100

```

```

JPI = J+1

```

```

KK = K-JPI

```

```

WRITE (6,120) JPI,K,KK

```

```

DO 110 I=JPI,K

```

```

110 DH(I) = FLOAT(M(I))

```



270  
280  
290  
300  
310  
320  
330  
340

```
C      CALL HISTO (0.,10.,20,T,KK,J,NODRW)
      CALL HISTO (0.,75.,15,S,KK,J,NODRW)
      CALL HISTO (0.,360.,36,DH,KK,J,NODRW)
      RETURN

C 120 FORMAT (2X,'DAILY HISTO FROM',I4,' TO ',I4,' TOTAL: ',I4,'PTS',//)
      END
```





# APPENDIX B: Program VECTOR DRAW

```

C C C
PROGRAM COMPOSITE DRAW PROVIDES A COMBINED TEMPERATURE, CURRENT
SPEED, AND CURRENT DIRECTION GRAPH.
10
20
30
40
50
60
70
80
90
100
110
120
130
140
150
160
170
180
190
200
210
220
230
240
250
260
270
280
290
300
310
320
330
340
350
360
370
380
390
400
410
420
430
440
450
460
470

DIMENSION T(5000), TIME(5000), S(5000), M(5000), A(5000), B(5000),
1 C(5000), TNEW(300)
REAL *8 IT, ITITLE(12)
REAL *8 JT, JTITLE(12)
REAL *8 KT, KTITLE(12)
REAL LABEL / 4H /
ND = NUMBER OF DATA SETS
INKTS=1 CONVERTS DATA IN KNOTS TO CM/SEC
READ (5,170) ND,INKTS
WRITE (6,180) ND
DO 160 J=1,ND
WRITE (6,190) J
NN = NUMBER OF DATA POINTS.
READ (5,200) NN
WRITE (6,210) NN
DEL IS THE SAMPLING INTERVAL IN HOURS.
DEL = 0.0833
WRITE (6,220) DEL
TIME(1) = 0
NODRW = 0
WRITE (6,230) NODRW
DO 100 I=1,NN,5
READ (5,240) (T(I+K-1),S(I+K-1),M(I+K-1),K=1,5)
CONTINUE
100
CCONVERT TO CM/SEC IF DATA INPUT IS IN KNOTS (INKTS=1).
IF (INKTS.NE.1) GO TO 120
DO 110 I=1,NN
110 S(I) = S(I)*51.479
120 CONTINUE
WRITE (6,250)
C

```







960  
970  
980  
990  
1000  
1010  
1020  
1030  
1040  
1050

```

190 FORMAT (//,5X,'DATA SET NUMBER',I4)
200 FORMAT (16)
210 FORMAT (//,5X,'NN =',1X,I4)
220 FORMAT (5X,'DEL =',1X,F7.4)
230 FORMAT (5X,'NODRW =',1X,I4)
240 FORMAT (5(F5.1,F5.2,I4))
250 FORMAT (//,1X,'DATA INPUT COMPLETED')
260 FORMAT (//,5X,'DATA CONVERTED FOR GRAPHICAL DISPLAY')
270 FORMAT (6A8)
      END

```



# APPENDIX C: Program COMPOSITE DRAW

```

PROGRAM VECTOR DRAW PROVIDES A PROGRESSIVE VECTOR DIAGRAM. THE
DIAGRAM REPRESENTS THE SUMMATION OF VECTORS MADE UP OF CURRENT
SPEED AND CURRENT DIRECTION FOR ONE HOUR PERIODS. INPUT VALUES
ARE OBTAINED FROM PROGRAM CURRENT. THE PROGRESSIVE VECTOR DIAGRAM
INDICATES THE NET TRANSPORT OF WATER AND ITS DIRECTION OF MOVEMENT

DIMENSION SPD(400), DIR(400), X(400), Y(400), A(400), B(400),
1 XA(400), YB(400)
REAL *8 IVT
REAL LABEL /4H /
REAL *8 ITITLE(12)
N = NUMBER OF DATA POINTS

READ (5,130) N
WRITE (6,140) N
READ (5,150) ITITLE
REAL *8 LABEA/8H/

READ IN DATA

READ (5,160) (SPD(I),DIR(I),I=1,N)

CONVERT SPEED DATA TO KNGTS

DO 100 I=1,N
100 SPD(I) = SPD(I)/51.479

PRINT OUT DATA

WRITE (6,170)
WRITE (6,180) (SPD(I),DIR(I),I=1,N)

INITILIZE

X(1) = 0.
Y(1) = 0.
A(1) = 0.
B(1) = 0.
N1 = N+1
WRITE (6,190)

DO 110 I=2,N1
110 I=2,N1

CONVERT DIRECTION IN DEGREES TO DIRECTION IN RADIAN BY

```









```

C      CONVERT TO METERS.
C      VECSUM = VECSUM*(1853.248)
C      WRITE (6,220) VECSUM
C
C      AREA = CNE SQUARE METER.
C      AREA = 1.0
C      WRITE (6,230) AREA
C
C      TOTAL VOLUME TRANSPORT IN CUBIC METERS.
C      TVT = AREA*VECSUM
C      WRITE (6,240) TVT
C
C      VOLUME TRANSPORT PER HOUR.
C      AN = N
C      XVT = TVT/AN
C      WRITE (6,250) XVT
C      STOP
C
130  FORMAT (I6)
140  FORMAT (1H1,6X,'NO. OF DATA POINTS = ',I6,///)
150  FORMAT (6A8)
160  FORMAT (8(F5.2,F4.0))
170  FORMAT (7X,'SPEED',3X,'DIRECTION',3X,'DATA PT. NO.',/)
180  FORMAT (5X,F5.2,6X,F4.0,9X,I4)
190  FORMAT (1H1)
200  FORMAT (5X,'X= ',F10.4,5X,'Y= ',F10.4,5X,'A= ',F10.4,5X,'B= ',
210  FORMAT (1H1,5X,'FINAL A VALUE= ',F10.4,1X,'N.M.',5X,'FINAL B VALUE
220  FORMAT (5X,'VECTOR SUM= ',F10.4,1X,'METERS',///)
230  FORMAT (5X,'AREA= ',F10.4,1X,'M**2',///)
240  FORMAT (5X,'TOTAL VOLUME TRANSPORT= ',1D20.13,1X,'M**3',///)
250  FORMAT (5X,'VOLUME TRANSPORT PER HOUR= ',F20.4,1X,'M**3/HR',///)
      END

```



## REFERENCES

- Caster, William A. 1969. Near-bottom currents in Monterey Submarine Canyon and on the adjacent shelf. M.S. thesis, Naval Postgraduate School, Monterey, Ca. 204 p.
- Dooley, J.J. 1968. Near bottom currents in Monterey Submarine Canyon. M.S. thesis, Naval Postgraduate School, Monterey, Ca. 58 p.
- E.G. & G., Inc., Waltham, Mass. Operating manual, Woods Hole Current Meter, Model A-100. Loose leaf. n.p.
- Gatje, P.H., and D.D. Pizinger. 1965. Bottom current measurements in the head of Monterey Submarine Canyon. M.S. thesis, Naval Postgraduate School, Monterey, Ca. 61 p.
- Hydro Products, Inc., San Diego, Ca. Operation and maintenance instructions for in-situ current speed, current direction and temperature recording system, Model 502. 49 p.
- Njus, J.J. 1968. Environmental factors affecting near-bottom currents in Monterey Submarine Canyon. M.S. thesis, Naval Postgraduate School, Monterey, Ca. 80 p.
- Richardson, W.S., P.B. Stimson, and C.H. Wilkins. 1963. Current measurements from moored buoys. Deep Sea Res. 10: 369-388.
- Shepard, F.P., R.R. Revelle, and R.S. Dietz. 1939. Ocean bottom currents off the California coast. Science 165: 177-178.
- Shepard, F.P. and R.F. Dill. 1966. Submarine canyons and other sea valleys. Rand McNally and Company, Chicago. 381 p.
- Shepard, F.P. 1967. Submarine canyon origin; based on deep-diving vehicle and surface ship operations. Revue de Geographie Physique et de Geographie Dynamique 9: 347-356.
- Shepard, F.P. and N.F. Marshall. 1969. Currents in La Jolla and Scripps Submarine Canyons. Science 165: 177-178.
- Shepard, F.P. and N.F. Marshall. 1973a. Storm generated current in La Jolla Submarine Canyon, California. Marine Geology 4: 19-24.



- Shepard, F.P. and N.F. Marshall. 1973b. Currents along floors of submarine canyons. Am. Assoc. Petroleum Geologists Bull. 57: 244-264.
- Shepard, F.P., N.F. Marshall, and P.A. McLoughlin. 1974a. Currents in submarine canyons. Deep Sea Res. 21: 691-706.
- Shepard, F.P., N.F. Marshall, and P.A. McLoughlin. 1974b. "Internal waves" advancing along submarine canyons. Science 183: 195-198.
- Webster, F. 1964a. Some perils of measurements from moored ocean buoys. Woods Hole Oceanographic Institution Reference No. 64-18. 16 p. Unpublished manuscript.
- Webster, F. 1964b. Processing moored current meter data. Woods Hole Oceanographic Institute Reference No. 64-55. 35 p. Unpublished manuscript.





# INITIAL DISTRIBUTION LIST

	No. Copies
1. Department of Oceanography, Code 58 Naval Postgraduate School Monterey, CA 93940	3
2. Dr. Robert S. Andrews Naval Postgraduate School Monterey, CA 93940	2
3. Lt. John E. Hollister, Code 3100 Naval Oceanographic Office Washington, DC 20373	2
4. Dr. Robert G. Paquette Naval Postgraduate School Monterey, CA 93940	2
5. Defense Documentation Center Cameron Station Alexandria, VA 22314	2
6. Library (Code 0212) Naval Postgraduate School Monterey, CA 93940	2
7. Dr. Alfred J. Carsola Lockheed Ocean Laboratory 3380 N. Harbor Drive San Diego, CA 92101	1
8. Dr. Francis P. Shepard Scripps Institution of Oceanography P.O. Box 1529 La Jolla, CA 92037	1
9. Dr. David Smith David D. Smith and Associates P.O. Box 429-E Pacific Beach, CA 92109	1
10. Dr. Robert E. Stevenson Scientific Liaison Office, ONR Scripps Institution of Oceanography La Jolla, CA 92037	1
11. Oceanographer of the Navy Hoffman II 200 Stoval Street Alexandria, VA 22332	1



- |     |   |   |
|-----|---|---|
| 12. | Library, Code 3330<br>Naval Oceanographic Office<br>Washington, DC 20373                                  | 1 |
| 13. | Office of Naval Research<br>Code 480<br>Arlington, VA 22217   | 1 |
| 14. | SIO Library<br>University of California, San Diego<br>P.O. Box 2367<br>La Jolla, CA 92037                 | 1 |
| 15. | Department of Oceanography Library<br>University of Washington<br>Seattle, WA 98105                       | 1 |
| 16. | Department of Oceanography Library<br>Oregon State University<br>Corvallis, OR 97331                      | 1 |
| 17. | Commanding Officer<br>Fleet Numerical Weather Central<br>Monterey, CA 93940                               | 1 |
| 18. | Commanding Officer<br>Environmental Prediction Research Facility<br>Monterey, CA 93940                    | 1 |
| 19. | Department of the Navy<br>Commander Oceanographic System, Pacific<br>Box 1390<br>FPO San Francisco, 96610 | 1 |













Thesis

162712

H686<sup>e</sup> Hollister

c.1      Currents in Monterey  
         Submarine Canyon.

thesH6865

Currents in Monterey Submarine Canyon.



3 2768 002 06919 7

DUDLEY KNOX LIBRARY